

El Niño and Southern Oscillation (ENSO): A Review

Chunzai Wang ¹

Clara Deser ²

Jin-Yi Yu ³

Pedro DiNezio ⁴

Amy Clement ⁵

¹ NOAA Atlantic Oceanographic and Meteorological Laboratory
Miami, Florida

² National Center for Atmospheric Research
Boulder, Colorado

³ University of California at Irvine
Irvine, California

⁴ International Pacific Research Center, University of Hawaii
Honolulu, Hawaii

⁵ Rosenstiel School of Marine and Atmospheric Science, University of Miami
Miami, Florida

A Chapter for Springer Book: *Coral Reefs of the Eastern Pacific*

May 2012

Corresponding author address: Dr. Chunzai Wang, NOAA/Atlantic Oceanographic and Meteorological Laboratory, 4301 Rickenbacker Causeway, Miami, FL 33149.
E-mail: Chunzai.Wang@noaa.gov.

Abstract

The ENSO observing system in the tropical Pacific plays an important role in monitoring ENSO and helping improve the understanding and prediction of ENSO. Occurrence of ENSO has been explained as either a self-sustained and naturally oscillatory mode of the coupled ocean-atmosphere system or a stable mode triggered by stochastic forcing. In either case, ENSO involves the positive ocean-atmosphere feedback hypothesized by Bjerknes. After an El Niño reaches its mature phase, negative feedbacks are required to terminate growth of the mature El Niño anomalies in the central and eastern Pacific. Four negative feedbacks have been proposed: reflected Kelvin waves at the ocean western boundary, a discharge process due to Sverdrup transport, western Pacific wind-forced Kelvin waves, and anomalous zonal advections. These negative feedbacks may work together for terminating El Niño, with their relative importance varying with time. Because of different locations of maximum SST anomalies and associated atmospheric heating, El Niño events are classified as eastern and central Pacific warming events. The identification of two distinct types of El Niño offers a new way to examine global impacts of El Niño and to consider how El Niño may respond and feedback to a changing climate. In addition to interannual variations associated with ENSO, the tropical Pacific SSTs also fluctuate on longer timescales. The patterns of Pacific Decadal Variability (PDV) are very similar to those of ENSO. When SST anomalies are positive in the tropical eastern Pacific, they are negative to the west and over the central North and South Pacific, and positive over the tropical Indian Ocean and northeastern portions of the high-latitude Pacific Ocean. Many mechanisms have been proposed for explaining PDV. Changes in ENSO under global warming are uncertain. Increasing greenhouse gases changes the mean states in the tropical Pacific which in turn induce ENSO changes. Due to the fact that the change in mean tropical condition under global warming is quite uncertain even during the past few decades, it is hard to say whether ENSO is going to intensify or weaken, but it is very likely that ENSO will not disappear in the future.

1. Introduction

El Niño is a large-scale oceanic warming in the tropical Pacific Ocean that occurs every few years. The Southern Oscillation is characterized by an interannual seesaw in tropical sea level pressure (SLP) between the western and eastern Pacific, consisting of a weakening and strengthening of the easterly trade winds over the tropical Pacific. Bjerknes (1969) recognized

that there is a close connection between El Niño and the Southern Oscillation (ENSO) and they are two different aspects of the same phenomenon. Bjerknes hypothesized that a positive ocean-atmosphere feedback involving the Walker circulation is a cause of ENSO (The Walker circulation consists of the surface trade winds blowing from the east to the west across the tropical Pacific Ocean, the rising air in the tropical western Pacific, the upper-level winds blowing from the west to the east, and the sinking air returned back to the surface in the tropical eastern Pacific). An initial positive sea surface temperature (SST) anomaly in the equatorial eastern Pacific reduces the east-west SST gradient and hence the strength of the Walker circulation (Gill, 1980; Lindzen and Nigam, 1987), resulting in weaker trade winds around the equator. The weaker trade winds in turn drive the ocean circulation changes that further reinforce SST anomaly. This positive ocean-atmosphere feedback leads the equatorial Pacific to a warm state, i.e., the warm phase of ENSO – El Niño. At that time, Bjerknes did not know what causes a turnabout from a warm phase to a cold phase, which has been named as La Niña (Philander, 1990).

After Bjerknes published his hypothesis, ENSO was not intensively studied until the 1980s. The intense warm episode of the 1982-83 El Niño, which was not recognized until it was well developed, galvanized the tropical climate research community to understand ENSO and ultimately predict ENSO. This motivated the ten-year international TOGA (Tropical Ocean-Global Atmosphere) program (1985-94) to study and predict ENSO. TOGA successfully built an ENSO observing system (McPhaden et al., 1998) and greatly advanced our understanding of ENSO by focusing on interaction between the tropical Pacific Ocean and atmosphere [e.g., see ENSO overviews by Philander (1990), Neelin et al. (1998), and Wang and Picaut (2004)].

After TOGA, the ENSO research community focused on different types of ENSO events, ENSO low-frequency variability and ENSO variability under global warming. All of these can change ocean temperatures in the tropical eastern Pacific which in turn affect coral reefs. For example, coral reefs in the tropical eastern Pacific experienced catastrophic coral mortality during the 1982/83 El Niño event (e.g., Glynn, 1985). Therefore, the understanding of ENSO-related ocean temperature variability in the tropical eastern Pacific is very important. This chapter provides a brief overview of ENSO studies. Section 2 briefly describes observations of ENSO. Section 3 reviews the understanding of ENSO mechanisms. Section 4 summarizes the recent development of the central versus eastern Pacific ENSO events. Section 5 reviews ENSO

low-frequency variations called Pacific decadal variability. Section 6 discusses ENSO variability under global warming. The chapter ends in Section 7 with a short summary.

2. ENSO observations

Modern observational data associated with ENSO can go back to the late 19th century. Because actual observations are sparse in the tropical Pacific during early period, data sets are normally produced using sparse observations, models, and statistical methods. Figure 1 shows ENSO indices from the beginning of the 20th century: The SST anomalies in the Nino3 region (150°W-90°W, 5°S-5°N) and Nino4 region (160°E-150°W, 5°S-5°N), and the zonal wind anomalies in the Nino4 region. Based on Fig. 1, several points can be made. First, the SST and zonal wind anomalies are highly correlated, indicating that ENSO is a coupled ocean-atmosphere phenomenon. Second, these ENSO indices show an oscillatory behavior with a 3-5 year preferred timescale, in spite of considerable irregularity in the oscillation. Third, ENSO events show asymmetry between El Niño warm events and La Niña cold events, with anomalies of El Niño larger than those of La Niña. Fourth, Fig. 1b shows that the central Pacific warm events (as represented by the Nino4 index) occur more frequently during the last few decades (see Section 4 for the detail). Another feature, which cannot be clearly seen in Fig. 1, is that ENSO is phase-locked to the seasonal cycle. That is, ENSO events tend to mature in the boreal winter (e.g., Rasmusson and Carpenter, 1982).

The variations of the thermocline are very important in ENSO events, but measurements of subsurface ocean temperature have been very sparse in the past. One of accomplishments for TOGA program was to build an ENSO observing system in the tropical Pacific Ocean. The backbone of the ENSO observing system is now called the TAO/TRITON array of about 70 moored buoys (Hayes et al., 1991; McPhaden, 1995) which is now supported and maintained by the U. S. and Japan. Most of them are equipped with a 500-m thermistor chain and meteorological sensors. At the equator five to seven moorings are equipped with ADCP (Acoustic Doppler Current Profiler) and current meters (McPhaden et al., 1998). Success of moored arrays in the tropical Pacific Ocean led to subsequent deployment of similar buoys in the tropical Atlantic and Indian Oceans (Fig. 2). The observed data are transmitted via satellites to data centers where they are compiled and made available to researchers and forecast centers in near-real time.

The evolution of El Niño and La Niña can be seen in the SST, zonal wind, and 20°C isotherm depth (a proxy for thermocline depth) anomalies of the TAO/TRITON array data along the equator. Here we use the 1997/98 El Niño event to demonstrate the evolution of the eastern Pacific warm event (see Section 4 for the detail of difference between the eastern and central Pacific warm events). The TAO/TRITON moored data in Fig. 3 show that there is a close relationship among zonal wind anomalies, SST anomalies and thermocline depth anomalies. The importance of subsurface variation is clearly seen. Even one year in advance of the maximum surface warming, the precursor of El Niño is visible subsurface in the western Pacific (with positive thermocline anomalies) associated with westerly wind anomalies. The depression of the thermocline extends slowly from the west to the east along the equator. When warm subsurface temperature anomalies caused by the thermocline deepening reach the east, they are carried by equatorial upwelling to the surface. Once SST becomes anomalously warm, the Bjerknes feedback begins. The westerly wind anomalies in the central Pacific cause the eastern Pacific thermocline to deepen further, inducing additional warming. However, when the surface water is warm in the eastern Pacific, the shallower thermocline is seen as subsurface cold anomalies in the western Pacific (Fig. 3). Even during the development of an El Niño event, the seeds of its destruction are being sown in the western Pacific. The eastward extension of the subsurface cold anomalies brings the gradual erosion of the surface warm anomalies. This initiates a reversal of the chain of the Bjerknes feedback, which acts to drive the coupled system into a La Niña event.

3. ENSO mechanisms

The theoretical explanations of ENSO can be loosely grouped into two frameworks. First, El Niño is one phase of a self-sustained, unstable, and naturally oscillatory mode of the coupled ocean-atmosphere system. Second, El Niño is a stable (or damped) mode triggered by or interacted with stochastic forcing or noise such as westerly wind bursts and Madden-Julian Oscillation events (e.g., Gebbie et al., 2007) and the tropical instability waves in the eastern Pacific Ocean (e.g., An, 2008). In either framework, ENSO involves the positive ocean-atmosphere feedback of Bjerknes (1969). The early idea of Wyrski's (1975) sea level "buildup" in the western Pacific warm pool treats El Niño as an isolated event. Wyrski suggested that prior to El Niño, the easterly trade winds strengthened, and there was a "buildup" in sea level in the western Pacific warm pool. A "trigger" is a rapid collapse of the easterly trade winds. When

this happens, the accumulated warm water in the western Pacific would surge eastward in the form of equatorial downwelling Kelvin waves to initiate an El Niño event.

3.1. Self-sustained oscillators of ENSO

Bjerknes (1969) first hypothesized that interaction between the atmosphere and the equatorial eastern Pacific Ocean causes El Niño. In Bjerknes' view, an initial positive SST anomaly in the equatorial eastern Pacific reduces the east-west SST gradient and hence the strength of the Walker circulation, resulting in weaker trade winds around the equator. The weaker trade winds in turn drive the ocean circulation changes that further reinforce the SST anomaly. This positive ocean-atmosphere feedback leads the equatorial Pacific to a never-ending warm state. A negative feedback is needed to turn the coupled ocean-atmosphere system around. However, during that time, it was not known what causes a turnabout from a warm phase to a cold phase. In search of necessary negative feedbacks for the coupled system, four conceptual ENSO oscillator models have been proposed: the delayed oscillator (Suarez and Schopf, 1988; Battisti and Hirst, 1989), the recharge oscillator (Jin, 1997a, b), the western Pacific oscillator (Weisberg and Wang, 1997; Wang et al., 1999), and the advective-reflective oscillator (Picaut et al., 1997). These oscillator models respectively emphasized the negative feedbacks of reflected Kelvin waves at the ocean western boundary, a discharge process due to Sverdrup transport, western Pacific wind-forced Kelvin waves, and anomalous zonal advection. These negative feedbacks may work together for terminating El Niño warming, as suggested by the unified oscillator (Wang, 2001).

3.1.1. The delayed oscillator

Suarez and Schopf (1988) introduced the conceptual delayed oscillator as a candidate mechanism for ENSO, by considering the effects of equatorially trapped oceanic wave propagation. Based on the coupled ocean-atmosphere model of Zebiak and Cane (1987), Battisti and Hirst (1989) formulated and derived a version of the Suarez and Schopf (1988) conceptual delayed oscillator model and argued that this delayed oscillator model could account for important aspects of the numerical model of Zebiak and Cane (1987). The positive ocean-atmosphere feedback occurs in the equatorial eastern Pacific, leading the Niño3 SST anomaly to a warm state. The delayed negative feedback is by free Rossby waves generated in the eastern

Pacific coupling region that propagate to and reflect from the ocean western boundary, returning as Kelvin waves to reverse the Niño3 SST anomalies in the eastern Pacific coupling region. The delayed oscillator assumes that the western Pacific is an inactive region for air-sea interaction and that ocean eastern boundary wave reflection is unimportant, emphasizing the importance of wave reflection at the ocean western boundary.

3.1.2. The recharge oscillator

Wyrtki (1975, 1985) first suggested a buildup in the western Pacific of warm water as a necessary precondition to the development of El Niño. Prior to El Niño upper ocean heat content or warm water volume over the entire tropical Pacific tends to build up (or charge) gradually, and during El Niño warm water is flushed toward (or discharged to) higher latitudes. After the discharge, the tropical Pacific becomes cold (La Niña) and then warm water slowly builds up again (recharge) before occurrence of next El Niño. The concept of the recharge and discharge processes is further emphasized by Jin (1997a, b). Based on the coupled model of Zebiak and Cane (1987), Jin (1997a, b) formulated and derived the recharge oscillator model. During the warm phase of ENSO, the divergence of Sverdrup transport associated with equatorial central Pacific westerly wind anomalies and equatorial eastern Pacific warm SST anomalies results in the discharge of equatorial heat content. The discharge of equatorial heat content leads to a transition phase in which the entire equatorial Pacific thermocline depth is anomalously shallow due to the discharge of equatorial heat content. This anomalous shallow thermocline at the transition phase allows anomalous cold waters to be pumped into the surface layer by climatological upwelling, leading to the cold phase. The converse occurs during the cold phase of ENSO. It is the recharge-discharge process that makes the coupled ocean-atmosphere system oscillate on interannual time scales.

3.1.3. The western Pacific oscillator

Observations show that ENSO displays both eastern and western Pacific interannual anomaly patterns (e.g., Rasmusson and Carpenter, 1982; Wang et al., 1999; Wang and Weisberg, 2000). During the warm phase of ENSO, warm SST anomalies in the equatorial eastern Pacific are accompanied by cold SST and shallow thermocline depth anomalies in the off-equatorial western Pacific. Also, while the zonal wind anomalies over the equatorial central Pacific are

westerly, those over the equatorial western Pacific are easterly. Consistent with these observations, Weisberg and Wang (1997) and Wang et al. (1999) developed a conceptual western Pacific oscillator model for ENSO. This model emphasizes the role of the western Pacific in ENSO that had been overlooked in the delayed oscillator. In particular, off-equatorial SST anomalies (and off-equatorial anomalous anticyclones) in the western Pacific induce equatorial western Pacific wind anomalies that affect the evolution of ENSO. Condensation heating due to convection in the equatorial central Pacific (e.g., Deser and Wallace, 1990) induces a pair of off-equatorial cyclones with westerly wind anomalies on the equator. These equatorial westerly wind anomalies act to deepen the thermocline and increase SST in the equatorial eastern Pacific, thereby providing a positive feedback for anomaly growth. On the other hand, the off-equatorial cyclones raise the thermocline there via Ekman pumping. Thus, a shallow off-equatorial thermocline anomaly expands over the western Pacific leading to a decrease in SST and an increase in SLP in the off-equatorial western Pacific (Wang et al., 1999; Wang, 2000). During the mature phase of El Niño, the off-equatorial anomalous anticyclones initiate equatorial easterly wind anomalies in the western Pacific. These equatorial easterly wind anomalies cause upwelling and cooling that proceed eastward as a forced ocean response providing a negative feedback, allowing the coupled ocean-atmosphere system to oscillate.

3.1.4. The advective-reflective oscillator

Picaut et al. (1997) proposed a conceptual advective-reflective oscillator model for ENSO. In this conceptual model, they emphasize a positive feedback of zonal currents that advect the western Pacific warm pool toward the east during El Niño. Three negative feedbacks tending to push the warm pool back to its original position of the western Pacific are: anomalous zonal current associated with wave reflection at the western boundary, anomalous zonal current associated with wave reflection at the eastern boundary, and mean zonal current converging at the eastern edge of the warm pool. During the warm phase of ENSO, equatorial westerly wind anomalies in the central Pacific produce upwelling Rossby and downwelling Kelvin waves that propagate westward and eastward, respectively. The westward propagating upwelling Rossby waves reflect as upwelling Kelvin waves after they reach the western boundary, whereas the eastward propagating downwelling Kelvin waves reflect as downwelling Rossby waves at the eastern boundary. Since both the upwelling Kelvin and downwelling Rossby waves have

westward zonal currents, they tend to push the warm pool back to its original position in the western Pacific. These negative feedbacks, along with the negative feedback of the mean zonal current, force the coupled ocean-atmosphere system to oscillate.

3.1.5. The unified oscillator

With several different conceptual oscillator models capable of producing ENSO-like oscillations, more than one may operate in nature. Motivated by existence of the above oscillator models, Wang (2001) formulated and derived a unified ENSO oscillator model from the dynamics and thermodynamics of the coupled ocean-atmosphere system that is similar to the Zebiak and Cane (1987) coupled model. Since ENSO is observed to show both eastern and western Pacific anomaly patterns, this oscillator model is formulated and constructed to consider SST anomalies in the equatorial eastern Pacific, zonal wind stress anomalies in the equatorial central Pacific, thermocline depth anomalies in the off-equatorial western Pacific, and zonal wind stress anomalies in the equatorial western Pacific. This model can oscillate on interannual timescales. The unified oscillator includes the physics of all oscillator models discussed above. All of the above ENSO oscillator models are special cases of the unified oscillator. As suggested by the unified oscillator, ENSO is a multi-mechanism phenomenon [see Picaut et al. (2002) for observations of different ENSO mechanisms] and the relative importance of different mechanisms is time-dependent.

3.2. A stable mode triggered by stochastic forcing

Another view of ENSO is that El Niños are a series of discrete warm events punctuating periods of neutral or cold conditions (La Niñas). That is, ENSO can be characterized as a stable (or damped) mode triggered by stochastic atmospheric/oceanic forcing (e.g., Lau, 1985; Pendland and Sardeshmukh, 1995; Moore and Kleeman, 1999; Philander and Fedorov, 2003; Kessler, 2003). This hypothesis proposes that disturbances external to the coupled system are the source of random forcing that drives ENSO. An attractive feature of this hypothesis is that it offers a natural explanation in terms of noise for the irregular behavior of ENSO variability. Since this view of ENSO requires the presence of “noise”, it easily explains why each El Niño is distinct and El Niño is so difficult to predict (e.g., Landsea and Knaff, 2000; Philander and Fedorov, 2003). The external atmospheric forcing may include the Madden-Julian Oscillation

and westerly wind bursts (e.g., Gebbie et al., 2007), and the oceanic noise may involve the tropical instability waves (e.g., An, 2008).

No matter whether El Niño is a self-sustained oscillator or a stable mode triggered by stochastic forcing, El Niño begins with warm SST anomalies in the equatorial central and eastern Pacific. After an El Niño reaches its mature phase, negative feedbacks are required to terminate growth of the mature El Niño anomalies in the central and eastern Pacific. In other words, the negative feedbacks of the delayed oscillator, the recharge oscillator, the western Pacific oscillator, and the advective-reflective oscillator may be still valid for demise of an El Niño, even if El Niño is regarded as a stable mode triggered by stochastic forcing. As discussed by Mantua and Battistti (1994), a sequence of independent warm events can still be consistent with delayed oscillator physics, since the termination of an individual El Niño event still requires negative feedback that can be provided by wave reflection at the western boundary.

4. Different flavors of ENSO events

It has been increasingly recognized that at least two different flavors or types of ENSO occur in the tropical Pacific (e.g., Wang and Weisberg, 2000; Trenberth and Stepaniak, 2001; Larkin and Harrison, 2005; Yu and Kao, 2007; Ashok et al., 2007; Kao and Yu, 2009; Kug et al., 2009). The two types of ENSO are the Eastern-Pacific (EP) type that has maximum SST anomalies centered over the eastern tropical Pacific cold tongue region, and the Central-Pacific (CP) type that has the anomalies near the International Date Line (Yu and Kao, 2007; Kao and Yu, 2009). The CP El Niño is also referred to as Date Line El Niño (Larkin and Harrison, 2005), El Niño Modoki (Ashok et al., 2007), or Warm Pool El Niño (Kug et al., 2009). As the central location of ENSO shifts, different influences or signatures may be produced in the eastern Pacific and corals. Therefore, it is important to know how these two types of ENSO differ in their structures, evolution, underlying dynamics, and global impacts.

4.1. Spatial structure and evolution of the Central-Pacific El Niño

The 1977/78 event is a typical example of the CP El Niño (Fig. 4b). During this El Niño, SST anomalies are mostly concentrated in the equatorial central Pacific from 160°E to 120°W, covering the Nino3.4 and Nino4 regions. In contrast, during the 1997/98 El Niño (Fig. 4a), which is a typical EP El Niño event, SST anomalies are mostly located in eastern part of the

tropical Pacific, extending from the South American coast around 80°W to 160°W and covering the Nino1+2 and Nino3 regions. Three distinct statistical methods have been used to identify the typical SST anomaly patterns of the EP and CP types of ENSO, including the standard Empirical Orthogonal Function (EOF) analysis of Ashok et al. (2007), the regression-EOF method of Kao and Yu (2009), and the composite analysis of Kug et al. (2009). The spatial patterns obtained by all three methods (Figs. 4c-h) for the two types of ENSO are similar. In particular, the CP ENSO patterns obtained by all three methods exhibit a poleward extension of SST anomalies from the central Pacific into both the northern and southern subtropics. The connection to the northern subtropics seems to be stronger, and the SST anomalies in the subtropical northeastern Pacific precede those in the equatorial central Pacific (Fig. 5). In addition, the propagating feature of the SST anomalies is weaker and less clear in the CP type of ENSO than in the EP type of ENSO. Below the ocean surface, while the EP ENSO is known to be characterized by subsurface temperature anomalies propagating across the Pacific basin (Fig. 3) similar to those described by the delayed oscillator theory of ENSO (Battisti and Hirst, 1989 and Schopf and Suarez, 1988), the CP ENSO is found to be associated more with subsurface ocean temperature anomalies that develop in-situ in the central Pacific (Fig. 6). The different subsurface evolution indicates that, in contrast to the EP ENSO, the underlying dynamics of the CP ENSO seems to be less dependent on thermocline variations (Kao and Yu, 2009; Kug et al., 2009).

In the atmosphere, wind stress and precipitation anomaly patterns associated with these two types of ENSO are also different. While the EP El Niño is associated with significant westerly anomalies covering a large part of the tropical Pacific, the westerly anomalies associated with the CP El Niño have a smaller spatial scale and are centered in the equatorial central-to-western Pacific (Kao and Yu, 2009; Kug et al., 2009). This more westward location of the westerly anomalies in the CP El Niño is consistent with the location of its SST anomalies. Significant easterly anomalies also appear over the tropical eastern Pacific during the CP El Niño. In terms of precipitation, positive anomalies associated with the EP El Niño typically extend from the equatorial eastern to central Pacific where the largest SST anomalies are located. For the CP El Niño, the precipitation anomalies are characterized by a dipole pattern, with positive anomalies located mainly in the western Pacific and negative anomalies in the eastern Pacific (Kao and Yu, 2009; Kug et al., 2009). The different precipitation patterns of these two types of ENSO imply

that the associated convective heating locations and the mid-latitude teleconnections could be different as well.

Several methods have been proposed to identify the two types of ENSO, which include using SST or subsurface ocean temperature information. Although there are some inconsistencies among the events identified by these various methods, there are several events commonly identified as the CP type by these methods, which include the following major El Niño events that have occurred since 1960s: 1968-69, 1977-78, 1986-87, 1991-92, 1994-95, 2002-03, 2004-05, and 2009-10. The 2009-10 El Niño is known to be one of the strongest CP El Niño events in the recent decades (Lee and McPhaden, 2010). This list reveals a tendency for the CP El Niño to occur more often in the recent decades (Ashok et al., 2007; Kao and Yu, 2009; Kug et al., 2009; Lee and McPhaden, 2010). It is interesting to note that at least three of the four El Niño events in the 21st century (i.e., the 2002/03, 2004/05, and 2009/10 events) have been of the CP type. Yeh et al. (2009) compared the ratio of the CP to EP type of El Niño events in Coupled Model Intercomparison Project phase 3 (CMIP3) model simulations and noticed that the ratio is projected to increase under a global warming scenario. They argued that the recent increase in the occurrence of the CP El Niño is related to a weakening of the mean Walker circulation and a flattening of the mean thermocline in the equatorial Pacific, which might be a result of global warming (Vecchi et al., 2007). However, it was also argued that the increasing occurrence of the CP El Niño in recent decades could be an expression of natural multidecadal variability and not necessarily a consequence of anthropogenic forcing (Newmann et al., 2011; McPhaden et al., 2011).

4.2. Dynamics of the Central-Pacific El Niño

A specific generation mechanism for the CP ENSO has yet to be fully agreed upon, and there are ongoing debates as to whether the CP ENSO should be considered as completely different entity from the EP ENSO or simply a different expression of the same EP ENSO dynamics. As mentioned, for the CP El Niño the equatorial westerly anomalies appear to the west of the positive SST anomalies in the central Pacific and the equatorial easterly anomalies to the east. Ashok et al. (2007) argued that the thermocline variations induced by this wind anomaly pattern are responsible for the generation of the CP ENSO. The equatorial westerly anomalies induce downwelling Kelvin waves propagating eastward and the equatorial easterly

anomalies induce downwelling Rossby waves propagating westward and, together, they deepen the thermocline in the central Pacific to produce the CP El Niño. Kug et al. (2009) emphasized the fact that the equatorial easterly anomalies can suppress warming in the eastern Pacific during a CP El Niño event by enhancing upwelling and surface evaporation. However, they also argued that the mean depth of thermocline in the central Pacific is relatively deep and the wind-induced thermocline variations may not be efficient in producing the CP SST anomalies. Instead, they suggested that ocean advection is responsible for the development of the central Pacific warming. A mixed-layer heat budget analysis performed by Yu et al. (2010) also concluded that the SST anomalies of the CP ENSO undergo rapid intensification through ocean advection processes. However, they argued that the initial establishment of the SST anomalies in the central equatorial Pacific is related to forcing from the extratropical atmosphere and subsequent atmosphere-ocean coupling in the subtropics. They suggested that SST anomalies appear first in the northeastern subtropical Pacific and later spread toward the central equatorial Pacific. The specific coupling processes in the subtropics responsible for the equatorward spreading are similar to those depicted by the seasonal footprinting mechanism (Vimont et al., 2001, 2003, 2009). This mechanism explains how wintertime mid-latitude atmospheric variations can force subtropical SST anomalies, sustain them from winter to the next summer, and at the same time spread them toward the central-to-western equatorial Pacific.

4.3. Distinct climate impacts of the Central-Pacific ENSO

The atmospheric response to SST anomalies can be sensitive to their exact location (e.g., Mo and Higgins, 1998; Hoerling and Kumar, 2002; Alexander et al., 2002; Basugli and Sardeshmukh, 2002; DeWeaver and Nigam, 2004). Several studies have indicated that the impacts of the CP ENSO could be distinctly different from those of the EP ENSO. For example, the impact of the CP ENSO on the U. S. winter temperatures has been found to be characterized by the well-known north-south dipole pattern associated with the EP ENSO but characterized by an east-west dipole pattern for the CP ENSO (Mo, 2010). The western North Pacific summer monsoon has a stronger relationship with the CP ENSO than the EP ENSO (Weng et al., 2011), and rainfall variations in southern China are different for the two types of ENSO (e.g., Feng and Li, 2011; Zhang et al., 2011). Australian rainfall has also been suggested to be more sensitive to the CP type than to the EP type of ENSO (Wang and Hendon, 2007; Taschetto and England,

2009). The results shown in Kumar et al. (2006) also imply that the CP El Niño can reduce the Indian monsoon rainfall more effectively than the EP El Niño. In the Southern Hemisphere, the CP ENSO has been shown to have a stronger impact on storm track activity than the EP ENSO (Ashok et al., 2007). The 2009 CP El Niño event was argued to have an influence far south as to contribute to the melting of Antarctica ice by inducing a stationary anticyclone outside the polar continent and enhancing the eddy heat flux into the region (T. Lee et al., 2010). The influence of the CP El Niño on Atlantic hurricanes may also be different from the conventional EP El Niño (Kim et al., 2009), but it has been shown that the anomalous atmospheric circulation in the hurricane main development region during the CP El Niño is similar to that during the EP El Niño (S.-K. Lee et al., 2010). Opposite impacts were noticed for the tropical cyclone activity in the western Pacific: the tropical cyclone frequency in the South China Sea increases during CP El Niño years but decreases during EP El Niño years (Chen, 2011). These distinctly climate impacts of the EP and CP ENSOs imply that they may leave different signatures in paleoclimate proxies worldwide including corals, which needs to be explored.

5. Pacific decadal variability

In addition to year-to-year variations associated with the ENSO phenomenon, SSTs in the tropical Pacific also fluctuate on timescales of decades and longer (e.g., Mantua et al., 1997; Zhang et al., 1997; Power et al., 1999; Deser et al., 2004; Guan and Nigam, 2008). These tropical Pacific decadal SST variations, henceforth referred to as “Pacific Decadal Variability” or PDV (also called the Pacific Decadal Oscillation, or PDO in the literature), are organized into large-scale spatial patterns with linkages to other ocean basins and to other climate parameters such as rainfall, wind, and cloudiness. In this section, we describe the geographical distribution and temporal characteristics of PDV, and discuss the mechanisms which contribute to PDV.

5.1. Geographical and temporal characteristics of PDV

Figure 7 shows maps of the standard deviation (σ SST) of SST fluctuations on timescales less than 8 years (referred to as interannual) and greater than 8 years (referred to as decadal) based on the Hadley Centre Sea Ice and SST version 1 (HadISST1) dataset (Rayner et al., 2003) for the period of 1900-2010. Similar results are also obtained with other data sets (not shown). Prior to computing the σ SST, the mean seasonal cycle was removed by subtracting the long-term

monthly means from each month and the trend was removed using a quadratic fit to the time series. The largest values of interannual σ SST (exceeding 1°C) occur along the equatorial Pacific and coastal Peruvian upwelling zones, with additional prominent maxima along the Gulf Stream, Kuroshio Current and coastal Argentina. The same regions exhibit high values of decadal σ SST but with weaker amplitude (0.4° - 0.6°C). Notably, the contrast between minimum and maximum values of σ SST is much less on decadal timescales compared to interannual, especially within the tropics. The ratio of decadal σ SST to interannual σ SST (the top panel of Fig. 7) reveals that decadal variability is comparable in magnitude to interannual variability throughout much of the tropical Pacific, except along the eastern equatorial upwelling zone where it is considerably weaker. Thus, decadal SST fluctuations are more readily apparent outside of the canonical ENSO region (often termed the Nino3.4 region).

To further illustrate this point, we show a sequence of SST time series for selected regions in the tropical Indo-Pacific arranged from the east to west (Fig. 8). The top panel shows the canonical ENSO region, and the remaining panels show regions where the ratio of decadal-to-interannual variability is a maximum (regions are outlined in Fig. 7 and latitude/longitude boundaries are given in the figure caption). The bottom panel shows the canonical PDV region in the central North Pacific (see Mantua et al., 1997). Unfiltered monthly SST anomalies are displayed as colored bars and low-pass filtered anomalies are shown as black curves; all time series have been quadratically detrended.

The regional SST records exhibit similarities and differences. Interannual fluctuations associated with ENSO are most readily evident in the eastern equatorial Pacific index, but also appear in the other records, albeit less prominently due to the enhanced low-frequency variability. Decadal and longer timescale fluctuations are most apparent in the central North Pacific and tropical Indian Ocean indices (note that these have opposite sign), but similar behavior is evident in the other records. These low-frequency variations are characterized by relatively cold conditions during approximately 1910-1925 and 1947-1976, and by relatively warm conditions during approximately 1926-1945 and 1977-1998; however, the exact timing of the warm and cold intervals varies with region (similar epochs are evident in the central North Pacific record but with opposite sign). In addition to these inter-decadal variations, shorter decadal-scale fluctuations are evident, especially in the northeastern Pacific and western equatorial Pacific indices but also in the other records to varying degrees. For example, the

1947-1976 cold epoch is punctuated by a warm interval in the 1960s, and the 1925-1946 warm epoch is interrupted by a cold interval in the 1930s. The time series shown in Fig. 8 illustrate the complex nature of low-frequency SST variations at a particular location, and highlight that some aspects of decadal variability are common to all regions while others are unique to a particular area.

EOF analysis (e.g., von Storch and Zwiers, 1999) is a standard statistical technique used to identify preferred patterns of temporal variability. Figure 9 shows the global SST anomaly pattern associated with the leading EOF of SST anomalies over the tropical Indo-Pacific (20°E-80°W, 30°N-30°S) based on unfiltered data (left) and 8-year low-pass filtered data (right). As before, results are based on quadratically detrended monthly anomalies from the HadISST1 dataset during 1900-2010. Although the EOF calculation was restricted to the tropical Indo-Pacific domain, the patterns are displayed globally by regressing the detrended monthly SST anomalies at each location upon the associated PC time series. These regression maps display the amplitude of the SST anomalies (°C) associated with a one standard deviation departure of the PC time series.

The EOF based on unfiltered data depicts ENSO and its global SST teleconnections, while that based on low-pass filtered data represents PDV (e.g., Mantua et al., 1997; Zhang et al., 1997; Power et al., 1999). These EOFs account for 49% and 52% of the unfiltered and low-pass filtered variance, respectively; compared to EOF2, which accounts for 10% and 13%, respectively). The ENSO and PDV patterns are very similar, not only over the tropical Indo-Pacific but also globally. In particular, when SST anomalies are positive in the tropical eastern Pacific, they are negative to the west and over the central North and South Pacific, and positive over the tropical Indian Ocean and northeastern portions of the high-latitude Pacific Ocean. The primary difference between the PDV and ENSO patterns is that PDV lacks the narrow equatorial Pacific maximum that is the hallmark of ENSO. For this reason, PDV is often referred to as a “broadened ENSO pattern” (e.g., Zhang et al., 1997; Vimont, 2005). It may also be noted that PDV resembles the areas of maximum decadal σ SST (recall Fig. 7). The unfiltered PC time series (colored bars in the bottom panel of Fig. 9) is dominated by the interannual sequence of ENSO events, while the low-pass filtered PC (black curve) highlights the decadal variability in the unfiltered PC. This decadal variability is similar to that described in connection with the regional SST time series shown in Fig. 8. However, the decadal PC record should not be

mistaken for the actual SST time series at a given location, which often shows more complex behavior (Fig. 8). Nor should the EOF pattern be assumed to represent the actual spatial distribution of SST anomalies during a given warm epoch (such as 1926-1945 and 1977-1998) or cold epoch (such as 1910-1925 and 1947-1976) due to additional sources of variability as documented in Deser et al. (2004). By design, EOF analysis oversimplifies the actual spatial and temporal characteristics of the data.

Rainfall patterns are affected by ENSO and PDV, as shown by the regression maps of monthly precipitation anomalies upon the SST PC time series based on unfiltered and low-pass filtered data in Fig. 10 (left and right panels, respectively). The top panels show results based upon the globally-complete but short satellite record since 1979 from the Global Precipitation Climatology Project (GPCP; Adler et al., 2003), and the bottom panels show results based upon the spatially-incomplete but longer (1900-1998) land station data records (Hulme et al., 1998). There is remarkable consistency between the two types of rainfall data where they overlap in space, lending confidence to the results. As for SST, the patterns of rainfall anomalies associated with ENSO and PDV are generally similar and consist of positive anomalies in the equatorial Pacific and negative anomalies over the maritime continent and the southwestern tropical Pacific. Smaller amplitudes of positive and negative rainfall anomalies occur in the eastern Indian Ocean and western tropical Atlantic, respectively. Regional precipitation time series since 1900 are shown in Deser et al. (2004).

5.2. Mechanisms of PDV

There is much ambiguity regarding the physical origin of PDV and whether it is separable from ENSO. Some studies suggest that PDV, unlike ENSO, is not a single physical phenomenon or “mode”, but a superposition of several phenomena including ENSO, random atmospheric variability, and oceanic processes (e.g., Newman et al., 2003; Vimont, 2005; Schneider and Cornuelle, 2005; Newman, 2007; Alexander, 2010). Others indicate that PDV is the result of deterministic ocean-atmosphere interactions between the tropical Indo-Pacific and higher latitudes of the Pacific Ocean that produce a preferred timescale, although the mechanisms put forth differ in terms of which latitudinal region is key [see the recent review of Liu (2012)]. Some research suggests that there is no preferred timescale for PDV, proposing instead that it reflects a first-order autoregressive (or “red noise”) process that is stochastically driven from

either the extratropical Pacific, the tropical Pacific, or both (Pierce, 2001; Dommenges and Latif, 2008; Dommenges, 2010; Clement et al., 2011). In this view, the limited temporal record from the instrumental data (~100-150 years) is not sufficient to provide robust evidence of a spectral peak in the power spectrum, although nominal timescales of about 20 and 50 years have been proposed (Minobe, 1997, 1999; Deser et al., 2004). Indeed, attempts at reconstructing PDV from a variety of paleoclimate proxy records fail to show a robust timescale before the instrumental era (e.g., Biondi et al., 2001; D'Arrigo et al., 2005). Perhaps the most important message emerging from studies of PDV is that analysis techniques that pre-suppose a particular timescale for PDV through band-pass or low-pass filtering may not be isolating any underlying physical phenomenon but simply sampling a continuum of low-frequency variability, albeit with a well-defined geographical pattern. This cautionary message does not preclude the importance of reconstructing PDV back in time from paleoclimate proxy records, but it may alter the interpretation of such reconstructions.

PDV as defined in this chapter is only one measure of low-frequency SST variability in the Pacific sector. Other recurring patterns include the “North Pacific mode” (Deser and Blackmon 1995; Nakamura et al., 1997; Barlow et al., 2001; Guan and Nigam, 2008), which is closely related to PDV albeit with less amplitude in the tropical Indo-Pacific, and a “North Pacific Gyre Oscillation mode” with connections to the central equatorial Pacific (Di Lorenzo et al., 2008). Recently, Messie and Chavez (2011) have suggested that PDV is a combination of the ENSO and North Pacific modes. Like PDV, whether these patterns are true physical modes is not well understood. PDV is generally poorly represented in coupled ocean-atmosphere climate models, particularly in terms of linkages between the tropics and extratropics (Lienert et al., 2011; Deser et al., 2012).

PDV and ENSO share many common features such as the spatial patterns although it is premature to state that PDV is oscillatory in nature. Not surprisingly, their mechanisms may also have some similarities. As summarized in Section 3, many oscillator concepts have been proposed for the oscillatory and self-sustained nature of ENSO. Several authors have extended three oscillator concepts of ENSO to explain the decadal variability in the tropical Pacific. Off-equatorial Rossby waves are at the root of the modified delayed action oscillator of White et al. (2003) and the recharge oscillator of Jin (2001a). Yu and Boer (2004) note the resemblance of

the ENSO western Pacific oscillator of Weisberg and Wang (1997) with their findings on decadal variability and heat content anomalies in the western North and South Pacific.

6. ENSO under global warming

The summary and discussion in the previous sections are all focused on studies based on modern data and models. In this section, we briefly describe ENSO from the point of views of global warming and paleoclimatic records.

6.1. Climate response of the equatorial Pacific to global warming

Paleoclimatic records suggest that the strong east-west SST contrast of the annual-mean conditions in the equatorial Pacific may not be a stable and permanent feature. Average SST contrast across the equatorial Pacific was about 2°C, much like during a modern El Niño event (Wara et al., 2005) and during the warm early Pliocene (~4.5 to 3.0 million years ago). This mean state may have occurred during the most recent interval with a climate warmer than today, suggesting that the equatorial Pacific could undergo similar changes as the Earth's warms up in response to increasing greenhouse gases.

Competing theories anticipate either a stronger or weaker east-west SST contrast in response to warming. The eastern Pacific would warm up more due to cloud feedbacks (Meehl and Washington, 1996), evaporation feedbacks (Knutson and Manabe, 1995), or a weakening of the Walker circulation (Vecchi and Soden, 2007). But, the ocean could also oppose warming in the east because increased stratification enhances the cooling effect of upwelling (Clement et al., 1996; Seager and Murtugudde, 1997). The balance between these processes is not known, therefore it is unclear whether the SST gradient will strengthen or weaken in the future. For instance, the SST signature of these mechanisms has been difficult to detect in the simulations, modern observations, or proxies. Modern observations do not show a robust pattern of El Niño-like warming (Vecchi et al., 2008; Deser et al., 2010) (Fig. 11), despite evidence for a weakening of tropical atmospheric circulation (Vecchi et al., 2006; Zhang and Song, 2006). However, there is robust evidence for warming of the eastern equatorial Pacific during the 20th Century (Bunge and Clarke, 2009). The tropical eastern Pacific SST trend may be also caused by the Atlantic warming (Kucharski et al., 2011) through the mechanisms of the Walker circulation across

equatorial South America or inter-basin SST gradient and ocean dynamics (Wang, 2006; Wang et al., 2009; Rodriguez-Fonseca et al., 2009).

Climate models project a weak reduction of the SST gradient into the 21st century (Knutson and Manabe, 1995; Collins et al., 2005; Meehl et al., 2007). The lack of robust evidence for El Niño-like warming in models and observations could be due to cancellation among the mechanisms listed above, especially among the enhanced warming due to slower currents driven by a weaker Walker circulation and the enhanced cooling due to a more stratified ocean (DiNezio et al., 2009). Moreover, due to basic equatorial dynamics the adjustment of the thermocline to changes in the trade winds renders the Bjerknes feedback ineffective to amplify an initial El Niño-like warming (DiNezio et al., 2010; Clarke, 2010). For these reasons, a “permanent El Niño” in response to global warming is very unlikely, even if the Walker circulation weakens. Instead, climate models indicate that the equatorial Pacific may just warm up slightly more than the tropics (Fig. 12) due to the effect of the weakening of the Walker circulation on equatorial currents and a differential in evaporative damping with the off-equatorial tropics (Liu et al., 2006; DiNezio et al., 2009).

6.2. Sensitivity of ENSO to global warming

Paleoclimate records and climate models overwhelmingly indicate that the Pacific will continue to be characterized by large seasonal and interannual variability as the Earth warms up. Seasonally-resolved tropical Pacific paleoclimate records from periods in the Earth’s history that were both warmer and colder than today show that interannual variability was present. Available Pliocene records, for example, show that ENSO frequency and amplitude were not significantly different from today (Watanabe et al., 2011; Scroxton et al., 2011). Moreover, glacial climate also exhibited large seasonal and interannual variability as suggested by isotopic measurements on individual forams at the Last Glacial Maximum (Koutavas and Joanidis, 2009), and coral records from prior glacial stages (Tudhope et al., 2001). No climate models have thus far been able to render ENSO inactive in either warmer (Huber and Caballero, 2003; Galeotti et al., 2010, von der Heydt et al., 2011) or cooler climates (Zheng et al., 2008).

Neither climate models and observations nor proxies provide a conclusive answer on whether ENSO is going to become stronger or weaker as the tropics warm up in response to increasing greenhouse gases (GHGs). Climate change simulations coordinated by the CMIP3

simulate a wide range of responses from weaker to stronger. Whether ENSO has changed due to recent observed warming is also controversial according to the observational record (e.g., Trenberth and Hoar, 1997; Harrison and Larkin, 1997; Rajagopalan et al., 1997). For these reasons, the Intergovernmental Panel on Climate Change (IPCC) Fourth Assessment Report (AR4) concluded that there is no consistent indication of discernible changes in ENSO amplitude in response to increasing GHGs (Meehl et al., 2007; Guilyardi et al., 2009).

The direct cause of ENSO changes in response to climate changes is generally not straightforward. For instance, the CMIP3 models largely agree in the response of the background ocean conditions over which ENSO variability occurs, but they do not agree on whether or not ENSO will strengthen (Fig. 13). The projected changes in the mean climate include a shoaled, less tilted, and sharper thermocline; weaker zonal currents; and weaker upwelling (Vecchi and Soden, 2007; DiNezio et al., 2009). ENSO theory indicates that any of these changes in the mean climate can lead to changes in ENSO amplitude.

Changes in ENSO amplitude have been attributed to changes in the depth and sharpness of the equatorial thermocline by theoretical, modeling, and observational studies. For instance, a sharper and deeper thermocline leads to weaker ENSO amplitude in a simple coupled ocean-atmosphere model (Fedorov and Philander, 2001). Observations, in contrast, suggest that the strong ENSO events in the 1980s and 1990s could be a result of a deepening of the thermocline after the 1976 climate shift (Guilderson and Schrag, 1998) or a sharper thermocline due to GHG related warming (Zhang et al., 2008). However, the observational evidence is not conclusive because: (1) there is evidence of strong ENSO activity before the 20th Century (e.g. Grove, 1988) and (2) ENSO has been relatively quiet during the first decade of the 21th Century despite continued warming.

Climate models exhibit a robust relationship between increased ENSO amplitude and a sharper equatorial thermocline (Meehl et al., 2001). This relationship explains why the previous generation ocean models, which had very diffuse thermoclines, simulated much weaker ENSO variability than observed. Conversely, a sharper thermocline has been invoked to explain the increase ENSO amplitude in some increasing GHG experiments (e.g., Timmermann et al., 1999; Park et al., 2009). All models participating in CMIP3 simulate a sharper thermocline in response to increasing GHGs, yet not all of them simulate a stronger ENSO. Other physical processes, such as the shoaling of the thermocline, weaker upwelling, or warmer mean SST could also have

an amplifying or damping effect on ENSO. Thus, it is reasonable to hypothesize that depending on the balance of these changes, ENSO could strengthen or weaken (e.g., Guilyardi et al., 2009; Vecchi and Wittenberg, 2010; Collins et al., 2010).

Climate model projections do not agree on whether ENSO will increase because the interaction of ENSO and changes in the mean climate lead to subtle changes in the ENSO feedbacks. The shoaling and sharpening of the thermocline enhances ENSO variability, but the warmer mean SST results in stronger atmospheric damping, thus weakening ENSO (van Oldenborgh et al., 2005; Kim and Jin, 2010). The weakening of the Walker circulation and the increased thermal stratification associated with the surface intensified ocean warming, both robust features of the climate projections play opposing roles. This interaction results fundamentally from weaker climatological upwelling, driven by a weaker Walker circulation, and a stronger subsurface zonal temperature gradient, associated with the surface intensified ocean warming. All models simulate these mechanisms, yet their net effect on ENSO is not equal leading to the wide range of ENSO responses (e.g., Fig. 13). Overall, these studies show that there is a substantial amount of cancellation among the effect of the changes in the different ENSO feedbacks. As a result, the sensitivity of ENSO simulations to increasing greenhouse gases is much reduced.

7. Summary

The ENSO observing system in the tropical Pacific plays an important role in monitoring ENSO and helping improve the understanding and prediction of ENSO. ENSO has been viewed as a self-sustained, naturally oscillatory mode or a stable mode triggered by stochastic forcing. For both views, ENSO involves the positive ocean-atmosphere feedback over the eastern tropical Pacific hypothesized by Bjerknes (1969). After an El Niño reaches its peak, a negative feedback is required for terminating a continued growth of El Niño. Different negative feedbacks have been proposed since the 1980s associated with a delayed oscillator, a recharge oscillator, a western Pacific oscillator, and an advective-reflective oscillator. These self-sustained oscillators respectively emphasize the negative feedbacks of wave reflection at the ocean western boundary, discharge of equatorial heat content, equatorial wind in the western Pacific, and zonal advection. As suggested by the unified oscillator, all of these negative feedbacks work together to terminate El Niños, and their relative importance is time-dependent. The issue of ENSO as a self-sustained

oscillation mode or a stable mode triggered by random forcing is not settled. It is possible that ENSO is a self-sustained mode during some periods, a stable mode during others, or a mode that is intermediate or mixed between the former and the latter. The predictability of ENSO is more limited if ENSO is a stable mode triggered by stochastic forcing than if ENSO is a self-sustained mode, because the former depends on random disturbances.

A recent development or focus for ENSO study is to separate ENSO into the EP and CP ENSO events. Because the locations of maximum SST anomalies (and associated atmospheric heating) are different, these two types of ENSO events have different climate and weather-related impacts on the globe. Mechanisms for causing different types of ENSO need to be further studied although some studies have proposed different physical processes of the CP ENSO from the EP ENSO. The identification of the two distinct types of El Niño offers a new way to consider how El Niño may respond and feedback to a changing climate. In addition to considering how climate changes may affect the amplitude and frequency of ENSO, we should also consider that the dominant type of ENSO might be altered as a result. There is still much to learn about the dynamics of the CP ENSO and what causes the type of ENSO to vary and alternate. Nevertheless, ENSO may be changing and there is a need to prepare for the possible emergence of a new dominant type of ENSO and to revise existing modeling and prediction strategies that were developed primarily for the conventional EP type of ENSO. It is unfortunate that there are only a few CP El Niño events available in the observations (less than 12 since the 1950s, depending on the way a CP event is defined). While much can still be learned from this limited number of events, we should look for assistance from long-term coupled climate model simulations, as well as paleoclimate records, to obtain a better understanding of the emerging CP type of El Niño.

Low-frequency SST variability in the Pacific sector is called PDV. The ENSO and PDV patterns are very similar, not only over the tropical Indo-Pacific but also globally. When SST anomalies are positive in the tropical eastern Pacific, they are negative to the west and over the central North and South Pacific, and positive over the tropical Indian Ocean and northeastern portions of the high-latitude Pacific Ocean. The primary difference between the PDV and ENSO patterns is that PDV lacks the narrow equatorial Pacific maximum that is the hallmark of ENSO. The temporal variations of PDV are characterized by relatively cold conditions in the tropics during approximately 1910-1925 and 1947-1976, and by relatively warm conditions during

approximately 1926-1945 and 1977-1998. There is much ambiguity regarding the physical origin of PDV and whether it is separable from ENSO. Some studies suggest that PDV, unlike ENSO, is not a single physical phenomenon or “mode”, but a superposition of several phenomena including ENSO, random atmospheric variability, and oceanic processes. Others indicate that PDV is the result of deterministic ocean-atmosphere interactions between the tropical Indo-Pacific and higher latitudes of the Pacific Ocean that produce a preferred timescale, although the mechanisms put forth differ in terms of which latitudinal region is key.

ENSO changes under global warming are uncertain. The tropical Pacific response to global warming has been suggested to be neither El Niño-like nor La Niña-like since the mechanisms for these changes are different from that of ENSO events – the Bjerknes feedback. Increasing greenhouse gases changes the background mean states in the tropical Pacific Ocean and atmosphere which in turn induce ENSO changes. However, the response of the mean states to increasing greenhouse gases is uncertain. For example, the tropical Pacific zonal SST contrast under global warming is reported to be either strengthened or weakened. The uncertainty in the eastern Pacific warming may be also caused by the Atlantic warming. Due to the fact that the change in tropical mean condition under global warming is quite uncertain even during the past few decades, it is hard to say whether ENSO is going to intensify or weaken, but it is very likely that ENSO will not disappear in the future.

Tropical warm waters are normally favorable for coral reef development and growth. However, extremely warm waters can result in coral mortality. A combination of ENSO interannual, decadal and anthropogenic variations can induce a large ocean temperature change in the tropical eastern Pacific which then affects coral reefs. As detailed in this chapter, significant advances have been made in ENSO since the past decades. However, there are many issues and uncertainties that still under debate and need to be further investigated. In particular, the improvement of our understanding and prediction of natural and anthropogenic ENSO variations is an important task for the ENSO community.

Acknowledgments. CW thanks Ms. L. Zhang for plotting Fig. 1 and helping modify Fig. 2 provided by Dr. M. McPhaden. CD would like to thank Dr. Toby Ault for useful discussions and Mr. Adam Phillips for technical assistance with the figures. We thank Dr. Paul Fiedler and an anonymous reviewer for their comments and suggestions. CW is supported by grants from

NOAA's Climate Program Office and the base funding of NOAA AOML. NCAR is sponsored by the National Science Foundation (NSF). JYY acknowledges the support from NSF Grant ATM-0925396 and NOAA-MAPP Grant NA11OAR4310102. The findings and conclusions in this report are those of the author(s) and do not necessarily represent the views of the funding agency.

References

- Adler, R. F., and Co-authors (2003). The Version 2 Global Precipitation Climatology Project (GPCP) Monthly Precipitation Analysis (1979-Present). *J. Hydrometeor.*, **4**, 1147-1167.
- Alexander, M. A., and Co-authors (2002). The atmospheric bridge: The influence of ENSO teleconnections on air-sea interaction over the global oceans. *J. Climate*, **15**, 2205–2231.
- Alexander, M. A. (2010). Extratropical Air-Sea Interaction, SST Variability and the Pacific Decadal Oscillation (PDO). *Climate Dynamics: Why does Climate Vary*, Editors D. Sun and F. Bryan, AGU Monograph #189, Washington D. C., 123-148.
- An, S.-I. (2008). Interannual variations of the tropical ocean instability wave and ENSO. *J. Climate*, **21**, 3680-3686.
- Ashok, K., and Co-authors (2007). El Niño Modoki and its possible teleconnection. *J. Geophys. Res.*, **112**, C11007, doi:10.1029/2006JC003798.
- Barlow, M., Nigam, S., Berbery, E. H. (2001). ENSO, Pacific decadal variability, and U.S. summertime precipitation, drought, and stream flow. *J. Climate*, **14**, 2105–28.
- Barsugli, J. J., and Sardeshmukh, P. D. (2002). Global atmospheric sensitivity to tropical SST anomalies throughout the Indo-Pacific basin. *J. Climate*, **15**, 3427-3442.
- Battisti, D. S., and Hirst, A. C. (1989). Interannual variability in the tropical atmosphere-ocean model: influence of the basic state, ocean geometry and nonlinearity. *J. Atmos. Sci.*, **45**, 1687-1712.
- Biondi, F., Gershunov, A., and Cayan, D. (2001). North Pacific decadal climate variability since AD 1661. *J. Climate*, **14**, 5–10.
- Bjerknes, J. (1969). Atmospheric teleconnections from the equatorial Pacific. *Mon. Weather Rev.*, **97**, 163-172.

- Bunge, L., and Clarke, A. J. (2009). A verified estimation of the El Nino index NINO3.4 since 1877. *J. Climate*, **22**(14), 3979-3992.
- Chen, G. (2011). How Does Shifting Pacific Ocean Warming Modulate on Tropical Cyclone Frequency over the South China Sea?. *J. Climate*, **24**, 4695–4700.
- Clarke, A. J. (2010). Analytical theory for the quasi-steady and low-frequency equatorial ocean response to wind forcing: The 'tilt' and 'warm water volume' modes. *J. Phys. Oceanogr.* **40**(1), 121-137.
- Clement, A. C., Baker, A. C. and Leloup, J. (2010). Patterns of tropical warming. *Nature Geosci.*, **3**, 8–9. doi:10.1038/ngeo728.
- Clement, A., DiNezio, P., and Deser, C. (2011). Rethinking the Ocean's Role in the Southern Oscillation. *J. Climate*, **24**, 4056-4072.
- Collins, M., and Coauthors (2005). El Nino- or La Nina-like climate change? *Clim. Dyn.*, **24**, 89–104.
- Collins, M., and Coauthors (2010). The impact of global warming on the tropical Pacific and El Niño. *Nat. Geosci.*, **3**, 391-397.
- Compo, G. P., and Coauthors, (2011). The Twentieth Century Reanalysis Project. *Quart. J. Roy. Meteor. Soc.*, **137**, 1–28.
- D'Arrigo, R., and Co-authors (2005). Tropical North Pacific climate linkages over the past four centuries. *J. Climate*, **18**, 5253-5265.
- Deser, C., and Wallace, J. M. (1990). Large-scale atmospheric circulation features of warm and cold episodes in the tropical Pacific. *J. Climate*, **3**, 1254-1281.
- Deser, C., and Blackmon, M. L. (1993). Surface climate variations over the north Atlantic Ocean during winter: 1900– 1989. *J. Climate*, **6**, 1743–53.
- Deser, C., Phillips, A. S., and Hurrell, J. W. (2004). Pacific interdecadal climate variability: linkages between the tropics and the North Pacific during boreal winter since 1900. *J. Climate* **17**, 3109–24.
- Deser, C., Phillips, A. S., and Alexander, M. A. (2010). Twentieth Century Tropical Sea Surface Temperature Trends Revisited. *Geophys. Res. Lett.*, **37**, L10701, doi:10.1029/2010GL043321.
- Deser, C., Phillips, and Co-authors (2012). ENSO and Pacific Decadal Variability in Community Climate System Model Version 4. *J. Climate*, in press.

- DeWeaver, E., and Sumant, N. (2004). On the Forcing of ENSO Teleconnections by Anomalous Heating and Cooling. *J. Climate*, **17**, 3225–3235.
- Di Lorenzo, E., and Co-authors (2008). North Pacific Gyre Oscillation links ocean climate and ecosystem change. *Geophys. Res. Lett.*, **35**, L08607; doi:10.1029/2007GL032838.
- DiNezio, P. N., Clement, A. C., Vecchi, G., Soden, B., Kirtman, B. and Lee, S.-K. (2009). Climate response of the equatorial Pacific to global warming. *J. Climate*, **22**, 4873-4892.
- Di Nezio, P. N., Clement, A. C. and Vecchi, G. A. (2010). Reconciling Differing Views of Tropical Pacific Climate Change. *Eos, Trans. AGU*, *91*(16), 141-142.
- Dommenget, D., and Latif, M. (2008). Generation of hyper climate modes. *Geophys. Res. Lett.*, **35**, L02706, doi:10.1029/2007GL031087.
- Dommenget, D. (2010). A slab ocean El Nino. *Geophys. Res. Lett.*, **37**, L20701, doi:10.1029/2010GL044888.1.
- Fedorov, A. V., and Philander, S. G. (2001). A Stability Analysis of Tropical Ocean–Atmosphere Interactions: Bridging Measurements and Theory for El Niño. *J. Climate*, **14**, 3086–3101.
- Feng, J., and Li, J. (2011). Influence of El Niño Modoki on spring rainfall over South China. *J. Geophys. Res.*, **116**, D13102, doi:10.1029/2010JD015160.
- Galeotti, S., and Co-authors (2010). Evidence for active ENSO in the late Miocene greenhouse climate. *Geology*, 1017.
- Gebbie, G., Eisenman, I., Wittenberg, A. T., and Tziperman, E. (2007). Modulation of westerly wind bursts by sea surface temperature: A semi-stochastic feedback for ENSO. *J. Atmos. Sci.*, **64**, 3281-3295.
- Gill, A. E. (1980). Some simple solutions for heat-induced tropical circulation. *Quarterly Journal of Royal Meteorological Society*, **106**, 447-462.
- Glynn, P. W. (1985). El Nino-associated disturbance to coral reefs and post disturbance mortality by *Acanthaster planci*. *Mar. Ecol. Prog. Ser.*, **26**, 295-300.
- Grove, R. (1988). Global Impact of the 1789-93 El Niño. *Nature*, **393**, 318–319.
- Guan, B., and Nigam, S. (2008). Pacific sea surface temperatures in the twentieth century: an evolution-centric analysis of variability and trend. *J. Climate*, **21**, 2790–809.
- Guilderson, T. P., and Schrag, D. P. (1998). Abrupt shift in subsurface temperatures in the tropical pacific associated with changes in El Niño. *Science*, **281**, 240–243.

- Guilyardi, E., and Co-authors (2009). Understanding El Niño in ocean-atmosphere general circulation models: Progress and challenges. *Bull. Amer. Met. Soc.*, **90**, 325-340.
- Harrison, D. E., and Larkin, N. K. (1997). Darwin sea level pressure, 1876–1996: Evidence for climate change? *Geophys. Res. Lett.*, **24**, 1775–1782.
- Hayes, S. P., Mangum, L., Picaut, J., Sumi, J. A., and Takeuchi, K. (1991). TOGA-TAO: A moored array for real-time measurements in the tropical Pacific Ocean. *Bulletin of the American Meteorological Society*, **72**, 339-347.
- Hoerling, M. P., and Kumar, A. (2002). Atmospheric response patterns associated with tropical forcing. *J. Climate*, **15**, 2184-2203.
- Holland, C. L., and Mitchum, G. T. (2003). Interannual volume variability in the tropical Pacific. *J. Geophys. Res.*, **108**, 3369, doi:10.1029/2003JC001835.
- Huber, M. and Caballero, R. (2003). Eocene El Nino: Evidence for robust tropical dynamics in the “hothouse”. *Science*, **299**, 877–881.
- Hulme, M., Osborn, T. J., and Johns, T. C. (1998). Precipitation sensitivity to global warming: Comparison of observations with HadCM2 simulations. *Geophys. Res. Lett.*, **25**, 3379–3382, doi:10.1029/98GL02562.
- Jin, F. F. (1997a). An equatorial ocean recharge paradigm for ENSO. Part I: Conceptual model. *J. Atmos. Sci.*, **54**, 811-829.
- Jin, F. F. (1997b). An equatorial ocean recharge paradigm for ENSO. Part II: A stripped-down coupled model. *J. Atmos. Sci.*, **54**, 830-847.
- Jin, F.-F., Kimoto, M., and Wang, X. (2001). A model of decadal ocean-atmosphere interaction in the North Pacific basin. *Geophys. Res. Lett.*, **28**, 1531-1534.
- Kao, H. Y., and Yu, J. Y. (2009). Contrasting Eastern-Pacific and Central-Pacific Types of ENSO. *J. Climate*, **22**, 615-632.
- Kessler, W. S. (2003). Is ENSO a cycle or a series of events? *Geophys. Res. Lett.*, **29** (23), 2125, doi:10.1029/2002GL015924.
- Kim, H.-M., Webster, P. J., and Curry, J. A. (2009). Impact of shifting patterns of Pacific Ocean warming on north Atlantic tropical cyclones. *Science*, **325**, 77-80.
- Kim, S.-T., and Jin, F.-F. (2010). An ENSO stability analysis. Part II: results from the twentieth and twenty-first century simulations of the CMIP3 models. *Clim. Dyn.*, **36**, 1609-1627.

- Koutavas, A., and Joanidis, S. (2009). El Niño during the last glacial maximum. *Geochimica et Cosmochimica Acta.*, **73**, A690-A690.
- Knutson, T. R. and Manabe, S. (1995). Time-mean response over the tropical Pacific to increased CO₂ in a coupled ocean-atmosphere model. *J. Climate*, **8**, 2181–2199.
- Kucharski, F., Kang, I.-S., Farneti, R., and Feudale, L. (2011). Tropical Pacific response to 20th century Atlantic warming. *Geophys. Res. Lett.*, **38**, L03702, doi:10.1029/2010GL046248.
- Kug, J.-S., Jin, F.-F., and An, S.-I. (2009). Two-types of El Niño events: Cold Tongue El Niño and Warm Pool El Niño. *J. Climate*, **22**, 1499-1515.
- Kumar, K. K., Rajagopalan, B., Hoerling, M., Bates, G., and Cane, M. (2006). Unraveling the Mystery of Indian Monsoon Failure During El Niño. *Science*, **314**, 115–119.
- Landsea, C. W., and Knaff, J. A. (2000). How much skill was there in forecasting the very strong 1997-98 El Niño? *Bulletin of the American Meteorological Society*, **81**, 2107-2119.
- Larkin, N. K., and Harrison, D. E. (2005). Global seasonal temperature and precipitation anomalies during El Niño autumn and winter, *Geophys. Res. Lett.*, **32**, L16705, doi:10.1029/2005GL022860.
- Lau, K. M. (1985). Elements of a stochastic-dynamical theory of the long-term variability of the El Niño-Southern Oscillation. *J. Atmos. Sci.*, **42**, 1552-1558.
- Lee, S.-K., Wang, C., and Enfield, D. B. (2010). On the impact of central Pacific warming event on Atlantic tropical storm activity. *Geophys. Res. Lett.*, **37**, L17702, doi:10.1029/2010GL044459.
- Lee, T., and McPhaden, M. J. (2010). Increasing intensity of El Niño in the central-equatorial Pacific. *Geophys. Res. Lett.*, **37**, L14603, doi:10.1029/2010GL044007.
- Lee, T., and Co-authors (2010). Record warming in the South Pacific and western Antarctica associated with the strong central-Pacific El Niño in 2009–10. *Geophys. Res. Lett.*, **37**, L19704, doi:10.1029/2010GL044865.
- Lienert, F., Fyfe, J. C., and Merryfield, W. J. (2011). Do Climate Models Capture the Tropical Influences on North Pacific sea surface temperature variability? *J. Climate*, in press.
- Lindzen, R. S., and Nigam, S. (1987). On the role of sea surface temperature gradients in forcing low-level winds and convergence in the Tropics. *J. Atmos. Sci.*, **44**, 2418-2436.

- Liu, Z., Vavrus, S. J., He, F., Wen, N., and Zhang, Y. (2006). Rethinking tropical ocean response to global warming: The enhanced equatorial warming. *J. Climate*, **18**, 4684–4700.
- Liu, Z. (2012). Dynamics of Interdecadal Climate Variability: An Historical Perspective. *J. Climate*, in press.
- Mantua, N. J., and Battisti, D. S. (1994). Evidence for the delayed oscillator mechanism for ENSO: The “observed” oceanic Kelvin mode in the far western Pacific. *J. Phys. Oceanogr.*, **24**, 691-699.
- Mantua, N. J., Hare, S. R., Zhang, Y., Wallace, J. M., and Francis, R. (1997). A Pacific interdecadal climate oscillation with impacts on salmon production. *Bull. Am. Meteorol. Soc.*, **78**, 1069–1079.
- McPhaden, M. J. (1995). The Tropical Atmosphere Ocean Array is completed. *Bull. Am. Meteor. Soc.*, **76**, 739-741.
- McPhaden, M. J., and Co-authors (1998). The Tropical Ocean-Global Atmosphere observing system: A decade of progress. *J. Geophys. Res.*, **103**, 14169-14240.
- McPhaden, M. J., Lee, T., and McClurg, D. (2011). El Niño and its relationship to changing background conditions in the tropical Pacific. *Geophys. Res. Lett.* **38**, L15709, doi:10.1029/2011GL048275.
- Meehl, G. A., and Co-authors (2001). Factors that affect the amplitude of El Niño in global coupled climate models. *Clim. Dyn.*, **17**, 515–526.
- Meehl, G. A., and Washington, W. M. (1996). El Niño-like climate change in a model with increased atmospheric CO₂ concentrations. *Nature*, **382**, 56–60.
- Meehl, G. A., and Coauthors (2007). Global Climate Projections. *Climate Change 2007: The Physical Science Basis. Contribution of Working Group I to the Fourth Assessment Report of the Intergovernmental Panel on Climate Change*. Cambridge University Press, 747–845.
- Messie, M. and Chavez, F. (2011). Global modes of sea surface temperature variability in relation to regional climate indices. *J. Climate*, **24**, 4314-4331.
- Minobe, S. (1997). A 50–70 year climatic oscillation over the North Pacific and North America. *Geophys. Res. Lett.*, **24**, 683–86.
- Minobe, S. (1999). Resonance in bidecadal and pentadecadal climate oscillations over the North Pacific: role in climatic regime shifts. *Geophys. Res. Lett.*, **26**, 855–58.

- Mo, K. C., and Higgins, R. W. (1998). Tropical convection and precipitation regimes in the western United States. *J. Climate*, **11**, 2404-2423.
- Mo, K. C. (2010). Interdecadal Modulation of the Impact of ENSO on Precipitation and Temperature over the United States. *J. Climate*, **23**, 3639–3656.
- Moore, A. M., and Kleeman, R. (1999). Stochastic forcing of the ENSO by the intraseasonal oscillation. *J. Climate*, **12**, 1199-1220.
- Nakamura, H, Lin, H. G., and Yamagata, T. (1997). Decadal climate variability in the North Pacific in recent decades. *Bull. Am. Meteorol. Soc.*, **78**, 2215–26.
- Neelin, J. D., and Co-Authors (1998). ENSO theory. *J. Geophys. Res.*, **103**, 14,262-14,290.
- Newman, M., Compo, G., and Alexander, M. A. (2003). ENSO-forced variability of the Pacific Decadal Oscillation. *J. Climate*, **16**, 3853–57.
- Newman, M. (2007). Interannual to decadal predictability of tropical and North Pacific sea surface temperatures. *J. Climate*, **20**, 2333–56.
- Newman, M., Shin, S.-I., and Alexander, M. A. (2011). Natural variation in ENSO flavors. *Geophys. Res. Lett.*, L14705, doi:10.1029/2011GL047658.
- Park, W., and Coauthors (2009). Tropical Pacific Climate and Its Response to Global Warming in the Kiel Climate Model. *J. Climate*, **22**, 71–92.
- Penland, C., and Sardeshmukh, P. (1995). The optimal growth of the tropical sea surface temperature anomalies. *J. Climate*, **8**, 1999-2024.
- Pierce, D. W. (2001). Distinguishing Coupled Ocean-Atmosphere Interactions from Background Noise in the North Pacific. *Prog. Oceanogr.*, **49**, 331-352.
- Philander, S. G. (1985). El Niño and La Niña. *J. Atmos. Sci.*, **42**, 2652-2662.
- Philander, S. G. (1990), *El Niño, La Niña, and the Southern Oscillation*, Academic Press, London, 289 pp.
- Philander, S. G., and Fedorov, A. (2003). Is El Niño sporadic or cyclic? *Annual Review of Earth and Planetary Sciences*, **31**, 579-594.
- Picaut, J., Masia, F., and du Penhoat, Y. (1997). An advective-reflective conceptual model for the oscillatory nature of the ENSO. *Science*, **277**, 663-666.
- Picaut, J., Hackert, E., Busalacchi, A. J., Murtugudde, R., and Lagerloef, G. S. E. (2002). Mechanisms of the 1997-1998 El Niño-La Niña, as inferred from space-based observations. *J. Geophys. Res.*, **107**, 10.1029/2001JC000850.

- Power, S. B., Casey, T., Folland, C., Colman, A., and Mehta, V. (1999). Interdecadal modulation of the impact of ENSO on Australia. *Clim. Dyn.*, **15**, 319–24.
- Rajagopalan, B., Lall, U., and Cane, M. A. (1997). Anomalous ENSO occurrences: An alternative view. *J. Climate*, **10**, 2351–2357.
- Rasmusson, E. M., and Carpenter, T. H. (1982). Variations in tropical sea surface temperature and surface wind fields associated with the Southern Oscillation/El Niño. *Monthly Weather Review*, **110**, 354–384.
- Rayner, N. A., and Co-authors (2003). Global analyses of sea surface temperature, sea ice, and night marine air temperature since the late nineteenth century. *J. Geophys. Res.*, **108** (D14), 4407; doi:10.1029/2002JD002670.
- Rodriguez-Fonseca, B., and Co-authors (2009). Are Atlantic Niños enhancing Pacific ENSO events in recent decades? *Geophys. Res. Lett.*, **36**, L20705, doi:10.1029/2009GL040048.
- Schneider, N., Cornuelle, B. D. (2005). The forcing of the Pacific Decadal Oscillation. *J. Climate*, **18**, 4355–73.
- Schopf, P. S., and Suarez, M. J. (1988). Vacillations in a coupled ocean-atmosphere model. *J. Atmos. Sci.*, **45**, 549–566.
- Scroton, N., and Co-authors (2011). Persistent El Niño–Southern Oscillation variation during the Pliocene Epoch. *Paleoceanography*, **26**, PA2215, doi:10.1029/2010PA002097.
- Seager, R., and Murtugudde, R. (1997). Ocean dynamics, thermocline adjustment and regulation of tropical SST. *J. Climate*, **10**, 521–539.
- Suarez, M. J., and Schopf, P. S. (1988). A delayed action oscillator for ENSO. *J. Atmos. Sci.*, **45**, 3283–3287.
- Taschetto, A. S., and England, M. H. (2009). El Niño Modoki impacts on Australian rainfall. *J. Climate*, **22**, 3167–3174.
- Timmermann, A., Oberhuber, J., Bacher, A., Esch, M., and Latif, M. (1999). Increased El Niño frequency in a climate model forced by future greenhouse warming. *Nature*, **398**, 694–696.
- Trenberth, K. E., and Hoar, T. J. (1997). El Niño and climate change. *Geophys. Res. Lett.*, **24**, 3057–3060.
- Trenberth, K. E., and Stepaniak, D. P. (2001). Indices of El Niño evolution. *J. Climate*, **14**, 1697–1701.

- Tudhope, A.W., and Co-authors (2001). Variability in the El Niño-Southern oscillation through a glacial-interglacial cycle. *Science*, **291**, 1511-1517.
- van Oldenborgh, G. J., Philip, S. Y., and Collins, M. (2005). El Niño in a changing climate: a multi-model study. *Ocean Sci.*, **1**, 81–95.
- Vecchi, G. A., and Co-authors (2006). Weakening of tropical Pacific atmospheric circulation due to anthropogenic forcing. *Nature*, **441**, 73–76.
- Vecchi, G. A., and Soden, B. J. (2007). Global warming and the weakening of the tropical circulation. *J. Climate*, **20**, 4316–4340.
- Vecchi, G. A., A. Clement, and B. J. Soden, 2008. Examining the tropical Pacific's response to global warming. *EOS, Trans. Amer. Geophys. Union*, **89**, 8183.
- Vecchi, G.A., and Wittenberg, A.T. (2010). El Niño and our future climate: where do we stand? *Wiley Interdisciplinary Reviews: Climate Change*, pp.1757-778 DOI: 10.1002/wcc.33
- Vimont, D., Battisti, D., and Hirst, A. (2001). Footprinting: A Seasonal Connection Between the Tropics and Mid-Latitudes. *Geophys. Res. Lett.*, **28**, 3923-3926.
- Vimont, D. J., Wallace, J. M., and Battisti, D. S. (2003). The seasonal footprinting mechanism in the Pacific: Implications for ENSO. *J. Climate*, **16**, 2668–2675.
- Vimont, D. J. (2005). The contribution of the interannual ENSO cycle to the spatial pattern of ENSO-like decadal variability. *J. Climate*, **18**, 2080–92.
- Vimont, D. J., Alexander, M., and Fontaine, A. (2009). Midlatitude Excitation of Tropical Variability in the Pacific: The Role of Thermodynamic Coupling and Seasonality. *J. Climate*, **22**, 518-534.
- Von der Heydt, A. S., Nnafie, A., and Dijkstra, H. A. (2011). Cold tongue/Warm pool and ENSO dynamics in the Pliocene. *Clim. Past Discuss.*, **7**, 997–1027, bdoi:10.5194/cpd-7-997-2011.
- von Storch, H., and Zwiers, F. W. (1999). *Statistical Analysis in Climate Research*. Cambridge, UK: Cambridge Univ. Press.
- Wang, C., Weisberg, R. H., and Virmani, J. I. (1999). Western Pacific interannual variability associated with the El Niño-Southern Oscillation. *J. Geophys. Res.*, **104**, 5131-5149.
- Wang, C., and Weisberg, R. H. (2000). The 1997-98 El Niño evolution relative to previous El Niño events. *J. Climate*, **13**, 488-501.
- Wang, C., (2000). On the atmospheric responses to tropical Pacific heating during the mature phase of El Niño. *J. Atmos. Sci.*, **57**, 3767-3781.

- Wang, C. (2001). A unified oscillator model for the El Niño-Southern Oscillation. *J. Climate*, **14**, 98-115.
- Wang, C., and Picaut, J. (2004). Understanding ENSO physics – A review. In C. Wang, S.-P. Xie, & J. Carton, *Earth's Climate: The Ocean-Atmosphere Interaction* (pp. 21-48). American Geophysical Union.
- Wang, C. (2006). An overlooked feature of tropical climate: Inter-Pacific-Atlantic variability. *Geophys. Res. Lett.*, **33**, L12702, doi: 10.1029/2006GL026324.
- Wang, C., Kucharski, F., Barimalala, R., and Bracco, A. (2009). Teleconnections of the tropical Atlantic to the tropical Indian and Pacific Oceans: A review of recent findings. *Meteorologische Zeitschrift*, **18**, 445-454.
- Wang, G., and Hendon, H. H. (2007). Sensitivity of Australian rainfall to inter-El Nino variations. *J. Climate*, **20**, 4211-4226.
- Wara, M. W., Ravelo, A. C. and Delaney, M. L. (2005). Permanent El Niño-like conditions during the Pliocene warm period. *Science*, **309**, 758–761.
- Watanabe, M., and Co-authors (2011). Permanent El Niño during the Pliocene warm period not supported by coral evidence. *Nature*, **471**, 209–211, doi:10.1038/nature09777.
- Weisberg, R. H., and Wang, C. (1997). A western Pacific oscillator paradigm for the El Niño-Southern Oscillation. *Geophys. Res. Lett.*, **24**, 779-782.
- Weng, H., Wu, G. Liu, Y., Behera, S. K. and Yamagata, T. (2011). Anomalous summer climate in China influenced by the tropical Indo-Pacific Oceans. *Clim Dyn.*, **36**, 769–782, DOI 10.1007/s00382-009-0658-9.
- White, W. B., Tourre, Y. M., Barlow, M., and Dettinger, M. (2003). A delayed action oscillator shared by biennial, interannual, and decadal signals in the Pacific basin. *J. Geophys. Res.*, **108**, 3070, doi10.1029/2002JC001490.
- Wyrtki, K. (1975). El Niño -- The dynamic response of the equatorial Pacific Ocean to atmospheric forcing. *J. Phys. Oceanogr.*, **5**, 572-584.
- Wyrtki, K. (1985). Water displacements in the Pacific and genesis of El Niño cycles. *J. Geophys. Res.*, **90**, 7129-7132.
- Yeh, S.-W., Kug, J.-S., Dewitte, B., Kirtman, B., and Jin, F.-F. (2009). Recent changes in El Niño and its projection under global warming. *Nature*, **461**, 511-515.

- Yu, B., and Boer, G. J. (2004). The role of the western Pacific in decadal variability. *Geophys. Res. Lett.*, **31**, L02204, doi:10.1029/2003GL018471.
- Yu, J.-Y., and Kao, H.-Y. (2007). Decadal Changes of ENSO Persistence Barrier in SST and Ocean Heat Content Indices: 1958-2001. *J. Geophys. Res.*, **112**, D13106, doi:10.1029/2006JD007654.
- Yu, J.-Y., Kao, H.-Y., and Lee, T. (2010). Subtropics-Related Interannual Sea Surface Temperature Variability in the Equatorial Central Pacific. *J. Climate*, **23**, 2869-2884.
- Zebiak, S. E., and Cane, M. A. (1987). A model El Niño-Southern Oscillation. *Monthly Weather Review*, **115**, 2262-2278.
- Zhang, M., and Song, H. (2006). Evidence of deceleration of atmospheric vertical overturning circulation over the tropical Pacific. *Geophys. Res. Lett.*, **33**, L12701, doi:10.1029/2006GL025942.
- Zhang, Q., Guan, Y., and Yang, H. (2008). ENSO amplitude change in observation and coupled models. *Adv. Atmos. Sci.*, **25**, 361–366.
- Zhang, W., Jin, F. , Li, J., and Ren, H. (2011). Contrasting impacts of two-type El Niño over the western north Pacific during boreal autumn. *J. Meteor. Soc. Jap.*, **89**, 563-569.
- Zhang, Y, Wallace, J. M., and Battisti, D. S. (1997). ENSO-like interdecadal variability. *J. Climate*, **10**, 1004–20.
- Zheng, W., Braconnot, P., Guilyardi, E., Merkel, U., and Yu, Y. (2008). ENSO at 6ka and 21ka from ocean–atmosphere coupled model simulations. *Clim. Dyn.*, **30**, 745-762.

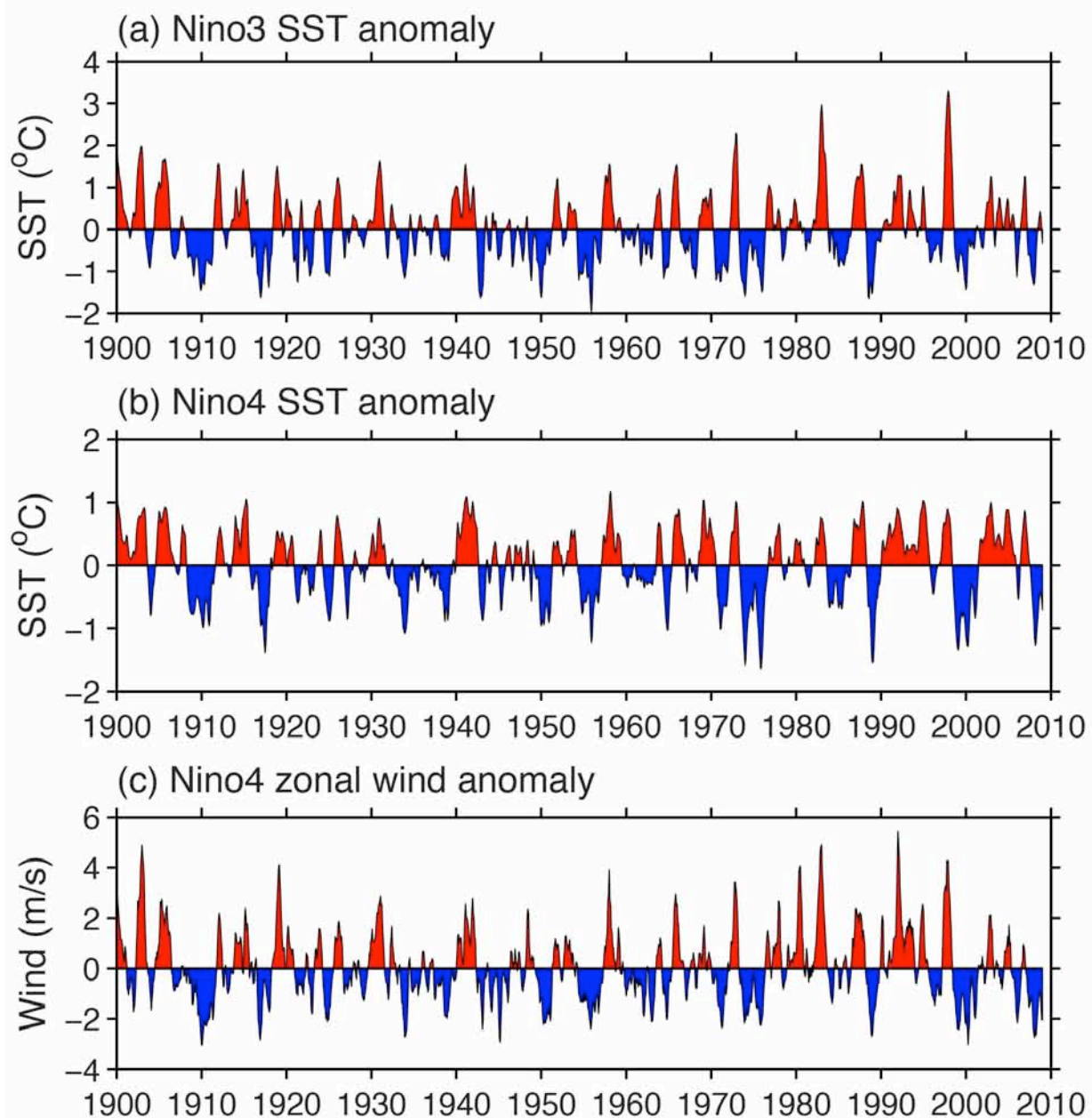


Figure 1. ENSO indices. Shown are (a) SST anomalies in the Nino3 region (5°S - 5°N , 150°W - 90°W), (b) SST anomalies in the Nino4 region (5°N - 5°S , 160°E - 150°W), and (c) zonal wind anomalies in the Nino4 region. All of the time series are three-month running means. SST is from the NOAA extended reconstructed SST version 3 (Smith et al. 2008) and wind is from the newly developed NOAA Earth System Research Laboratory (ESRL) 20th Century Reanalysis (20CR) (Compo et al. 2011).

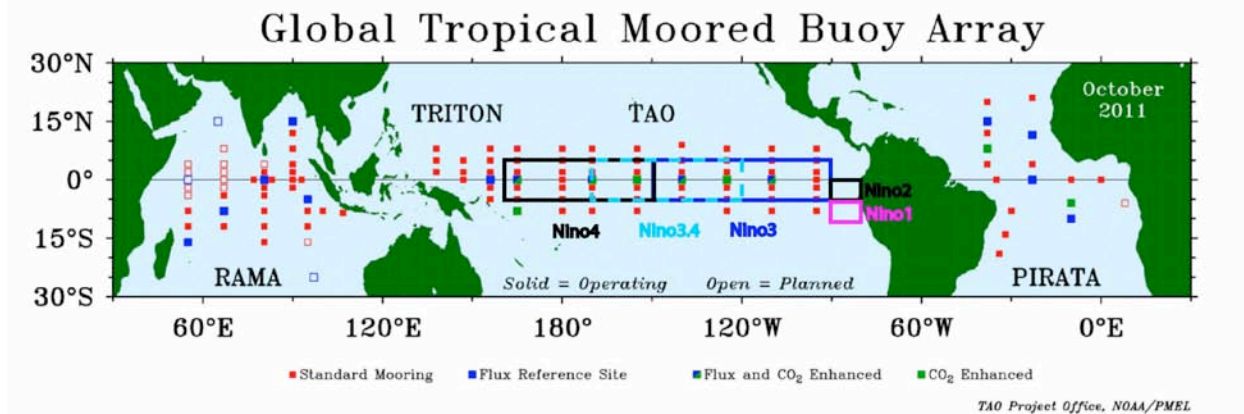


Figure 2. The global tropical moored buoy array. The ENSO observed array in the tropical Pacific is called the TAO/TRITON array. The instruments deliver, in near-real time, data on surface and subsurface temperature and salinity, wind speed and direction, current velocity and air-sea fluxes. Boxes outline the Nino3 region of 150°W-90°W, 5°S-5°N, the Nino4 region of 160°E-150°W, 5°S-5°N, the Nino3.4 region of 170°W-120°W, 5°S-5°N, the Nino1 region of 90°W-80°W, 5°S-10°S, and the Nino2 region of 90°W-80°W, 0°-5°S. The figure is modified from the one provided by Dr. Michael McPhaden at NOAA/PMEL.

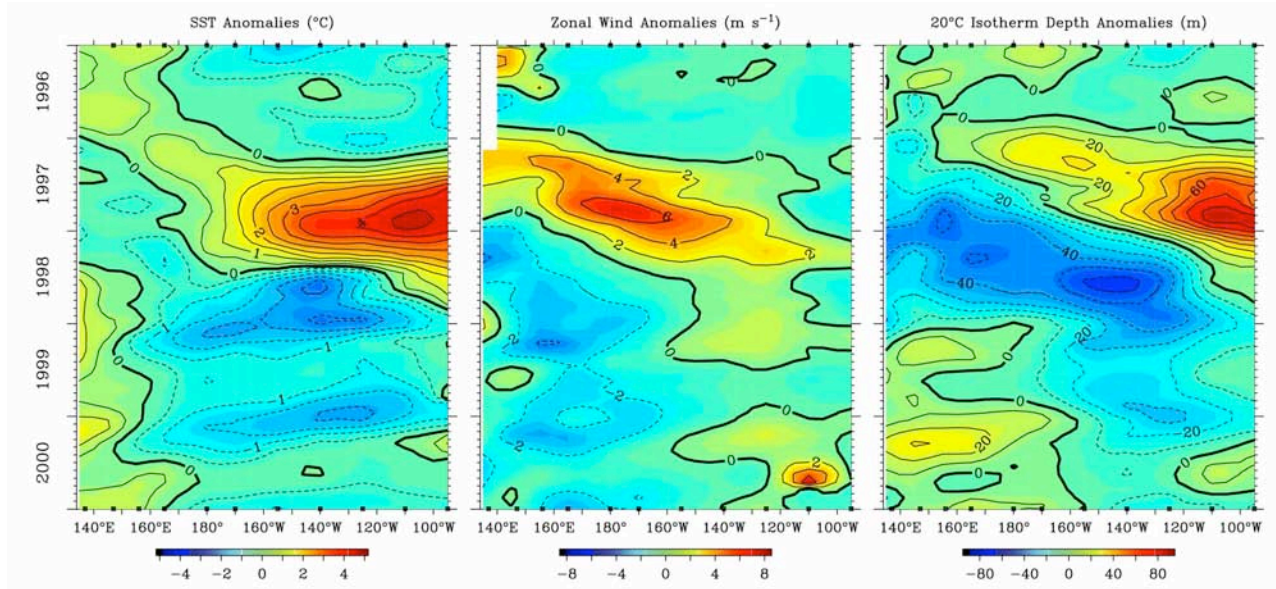


Figure 3. Time-longitude sections of monthly SST, zonal wind, and 20°C isotherm depth anomalies between 2°S to 2°N from January 1996 to December 2000. The data are provided by the TAO/TRITON array.

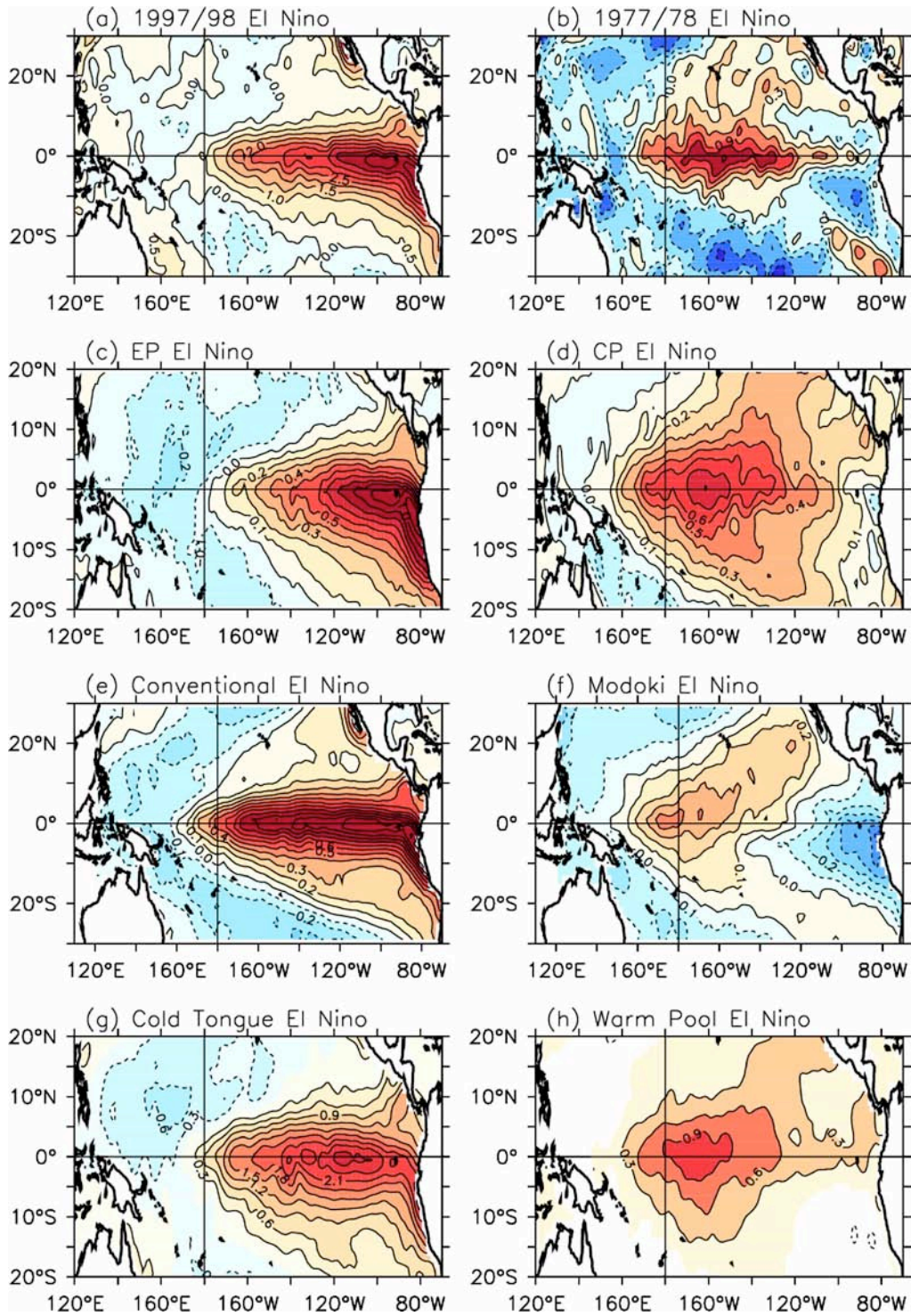


Figure 4. SST anomaly patterns for (a) the 1997-98 El Niño (anomalies averaged from November 1997 to January 1998); (b) the 1977-78 El Niño (anomalies averaged from November 1977 to January 1978); (c)-(d) the EP-ENSO and CP-ENSO obtained from the EOF-regression method of Kao and Yu (2009); (e)-(f) the 1st and 2nd EOF that representing the conventional El Niño and El Niño Modoki obtained from the regular EOF analysis of Ashok et al. (2007); and (g)-(h) the Cold Tongue and Wam Pool El El Niño composed by Kug et al. (2009). SST data from HadISST (1970-2005) is used for the calculation.

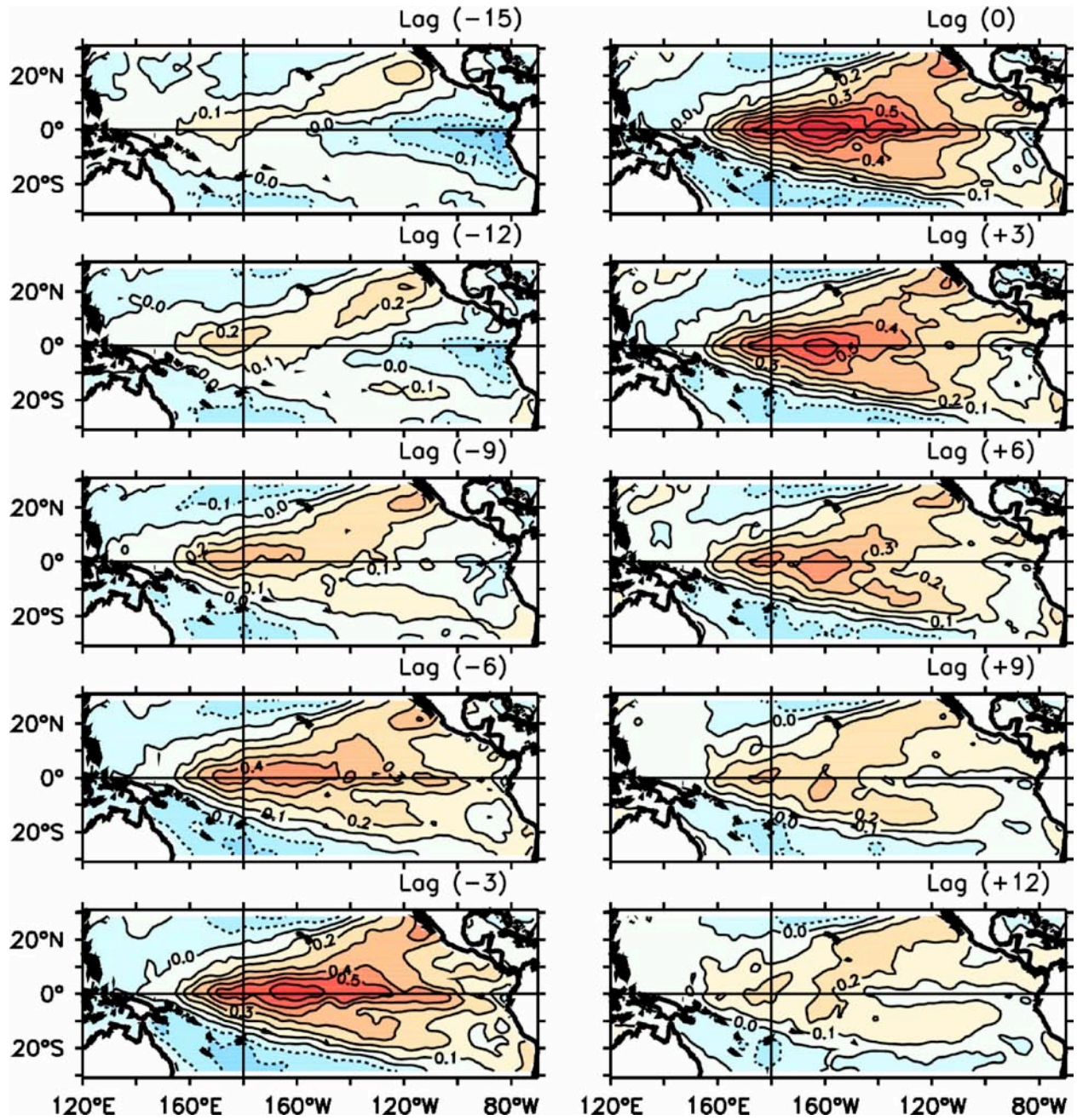


Figure 5. Evolution of SST anomalies of the CP ENSO. Values shown are the lagged (in months) correlation coefficients between the principal components of the CP-ENSO obtained from the EOF-regression method of Kao and Yu (2009) and tropical Pacific SST anomalies. Contour intervals are 0.1.

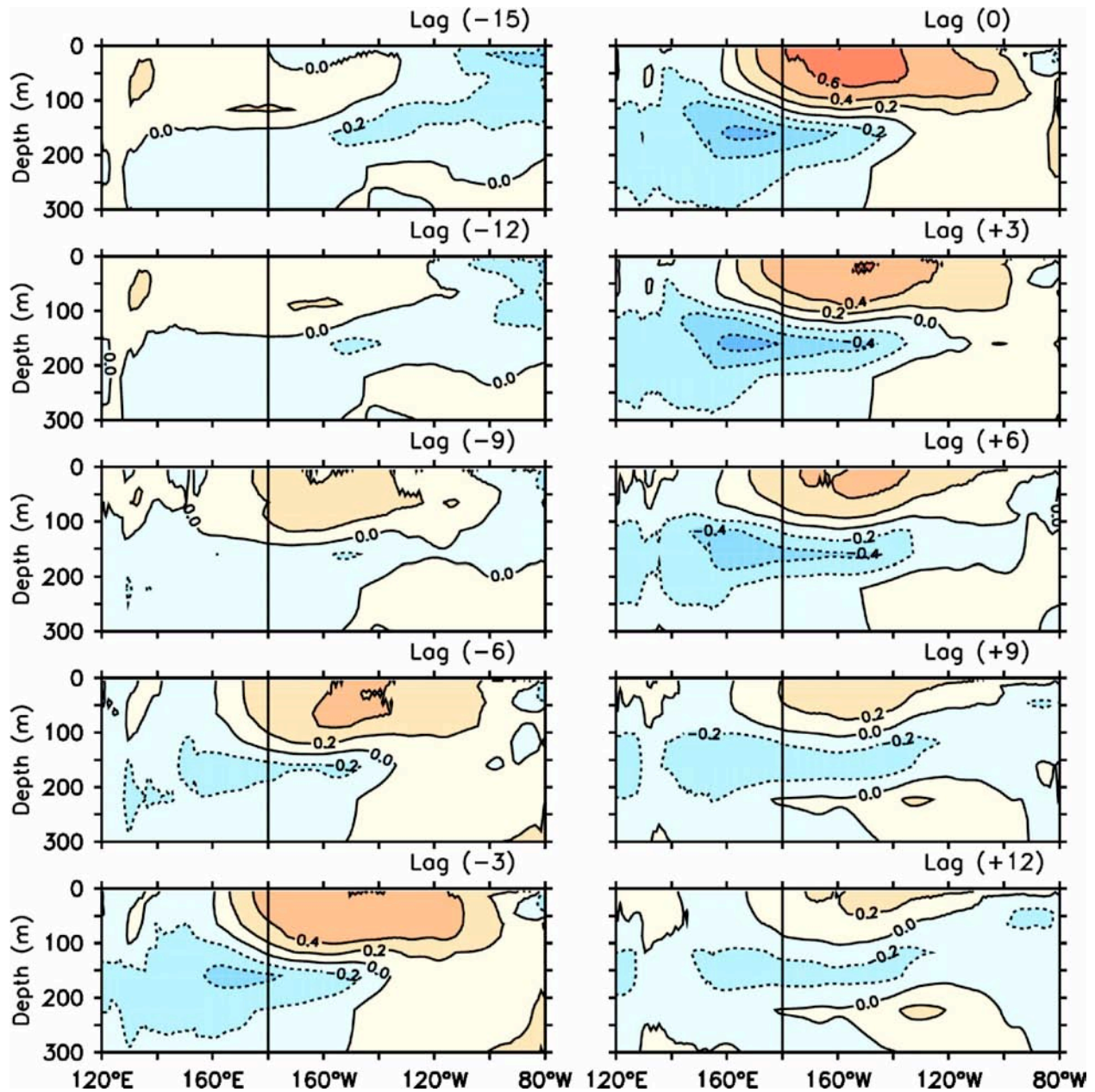


Figure 6. Evolution of subsurface ocean temperature anomalies of the CP ENSO along the equator (5°S-5°N). Values shown are the lagged correlation coefficients between the principal components of the CP ENSO obtained from the EOF-regression method of Kao and Yu (2009) and temperature anomalies. Contour intervals are 0.2. Ocean temperature assimilation from GECCO (1970-2001) is used for the calculation.

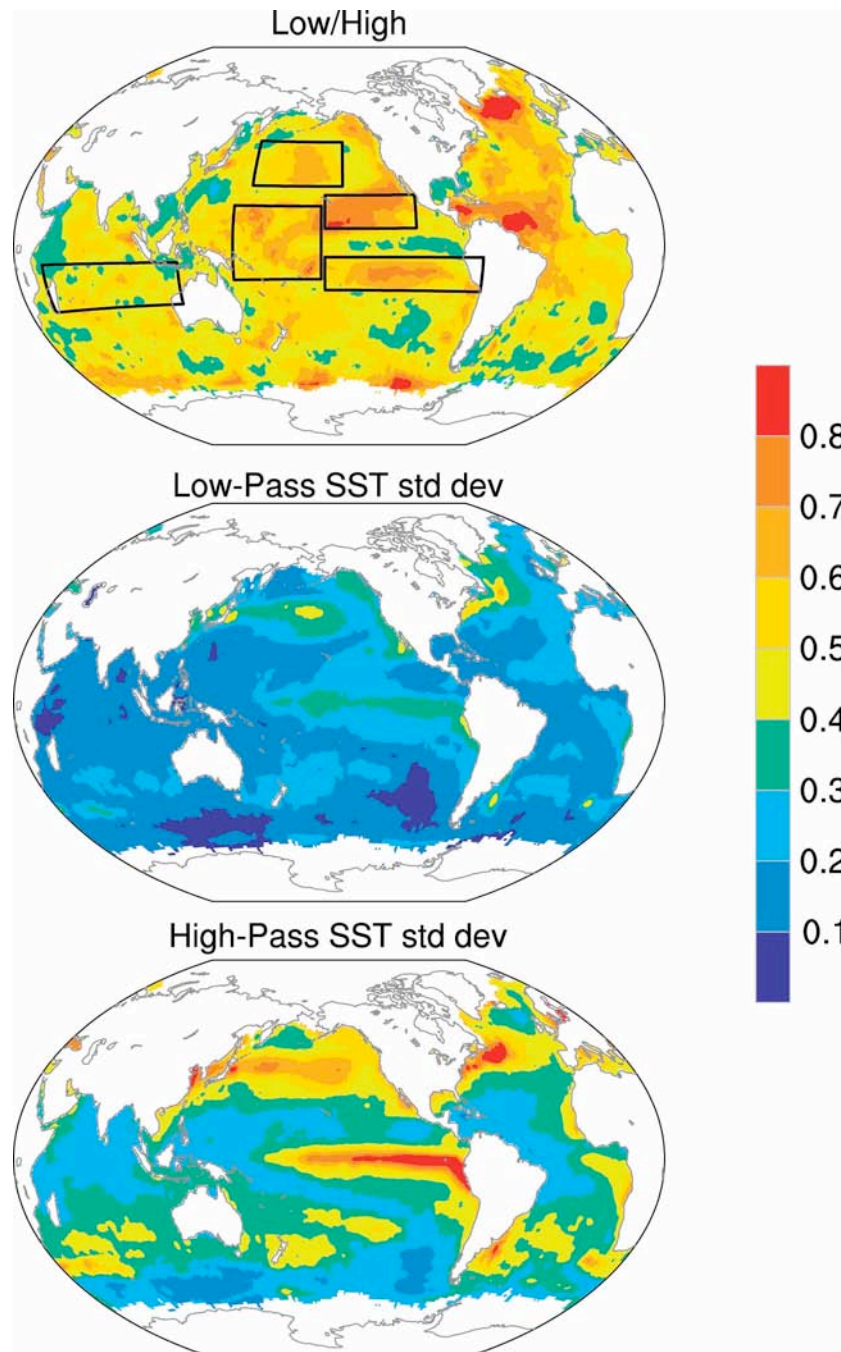


Figure 7. The standard deviation ($^{\circ}\text{C}$) of SST fluctuations on time scales less than 8 years (bottom panel) and greater than 8 years (middle panel) based on the HadISST1 dataset (Rayner et al., 2003) for the period 1900-2010 using the filter in Zhang et al. (1997). Prior to computing the standard deviations, the mean seasonal cycle was removed by subtracting the long-term monthly means from each month and the trend was removed using a quadratic fit to the time series. The top panel shows the ratio between the middle panel and the bottom panel. Boxes outline regions used in Fig. 8.

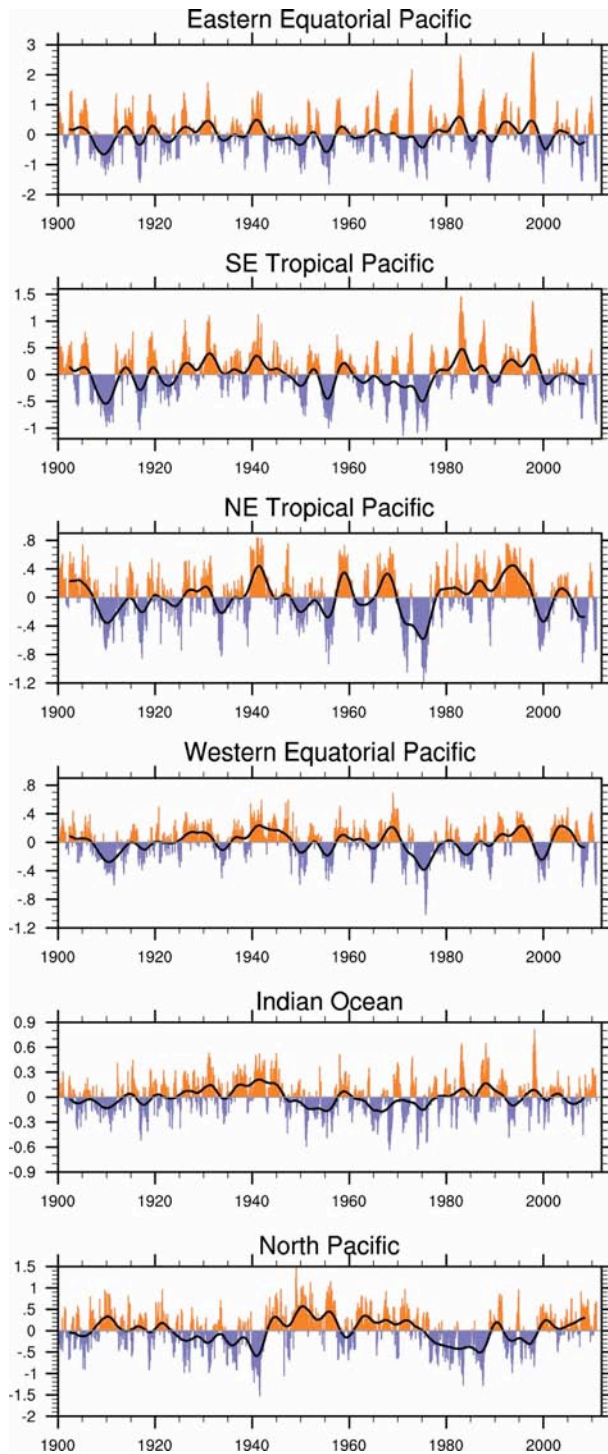


Figure 8. Regional SST time series in the tropical Indo-Pacific, arranged from the east to west (regions are outlined in the top panel of Fig. 7). Unfiltered monthly SST anomalies are displayed as colored bars and low-pass filtered anomalies are shown as black curves; all time series have been quadratically detrended. Regions are defined as follows: Eastern Equatorial Pacific (5°N - 5°S , 160°W - 90°W); SE Tropical Pacific (5°S - 20°S , 160°W - 70°W); NE Tropical Pacific (5 - 20°N , 160°E - 110°W); Western Equatorial Pacific (15°S - 15°N , 150°E - 160°W); Indian Ocean (5°S - 25°S , 45°E - 120°E); North Pacific (25°N - 45°N , 160°E - 150°W).

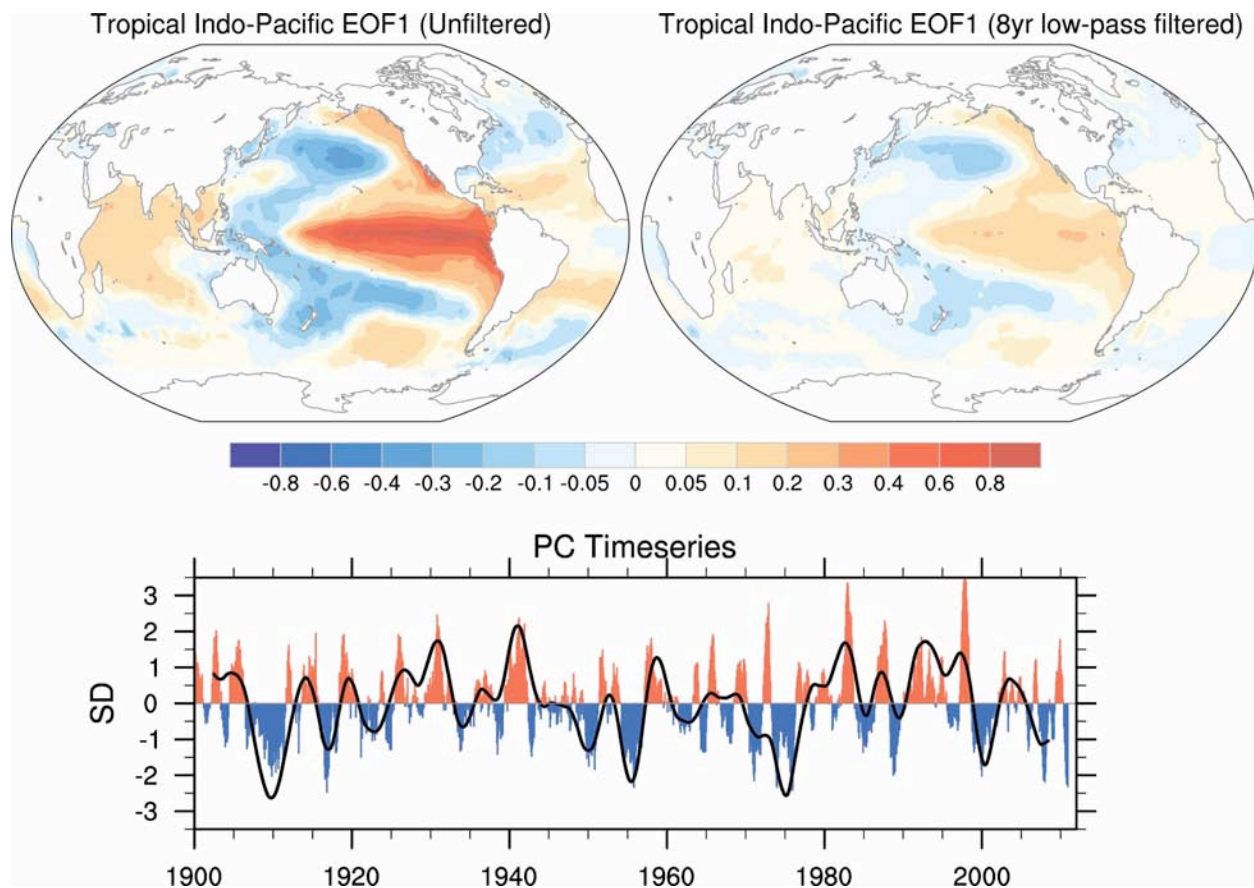


Figure 9. (Top panels) Global SST anomaly pattern associated with the leading EOF of SST anomalies over the tropical Indo-Pacific (30°N - 30°S , 20°E - 80°W) based on unfiltered data (left) and 8-year low-pass filtered data (right) based on quadratically detrended monthly anomalies from the HadISST1 dataset during 1900-2010. Units are $^{\circ}\text{C}$ per standard deviation of the PC time series. (Bottom panel) Standardized PC time series (colored bars for unfiltered data and black curve for low-pass filtered data).

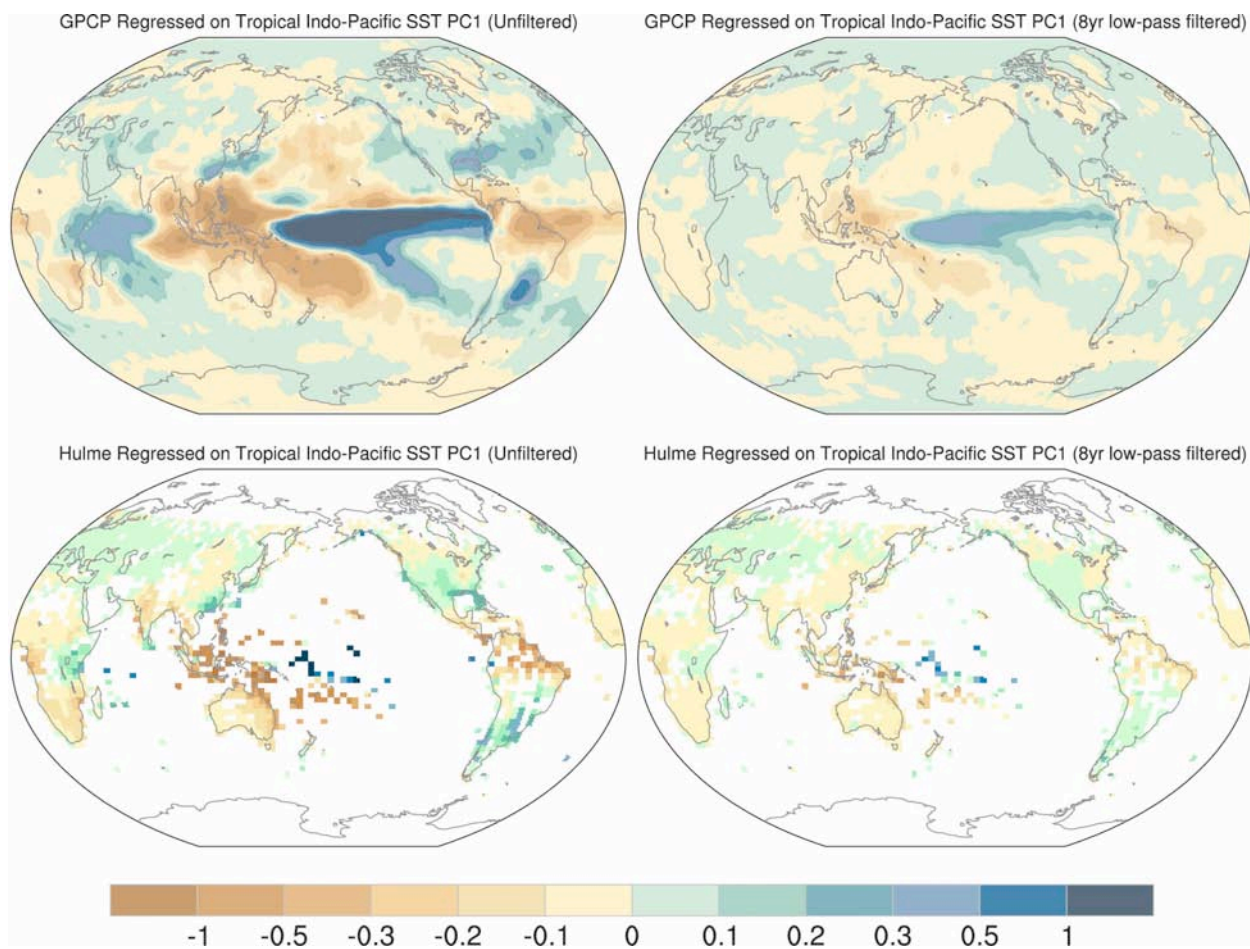


Figure 10. Regression maps of monthly precipitation anomalies upon the SST PC time series based on unfiltered and low-pass filtered data in Fig. 9 (left and right panels, respectively). The top panels show results based upon the satellite-based Global Precipitation Climatology Project for the period 1979-2011; bottom panels show results based upon land station data records during 1900-1998. Units are mm/day per standard deviation of the PC time series.

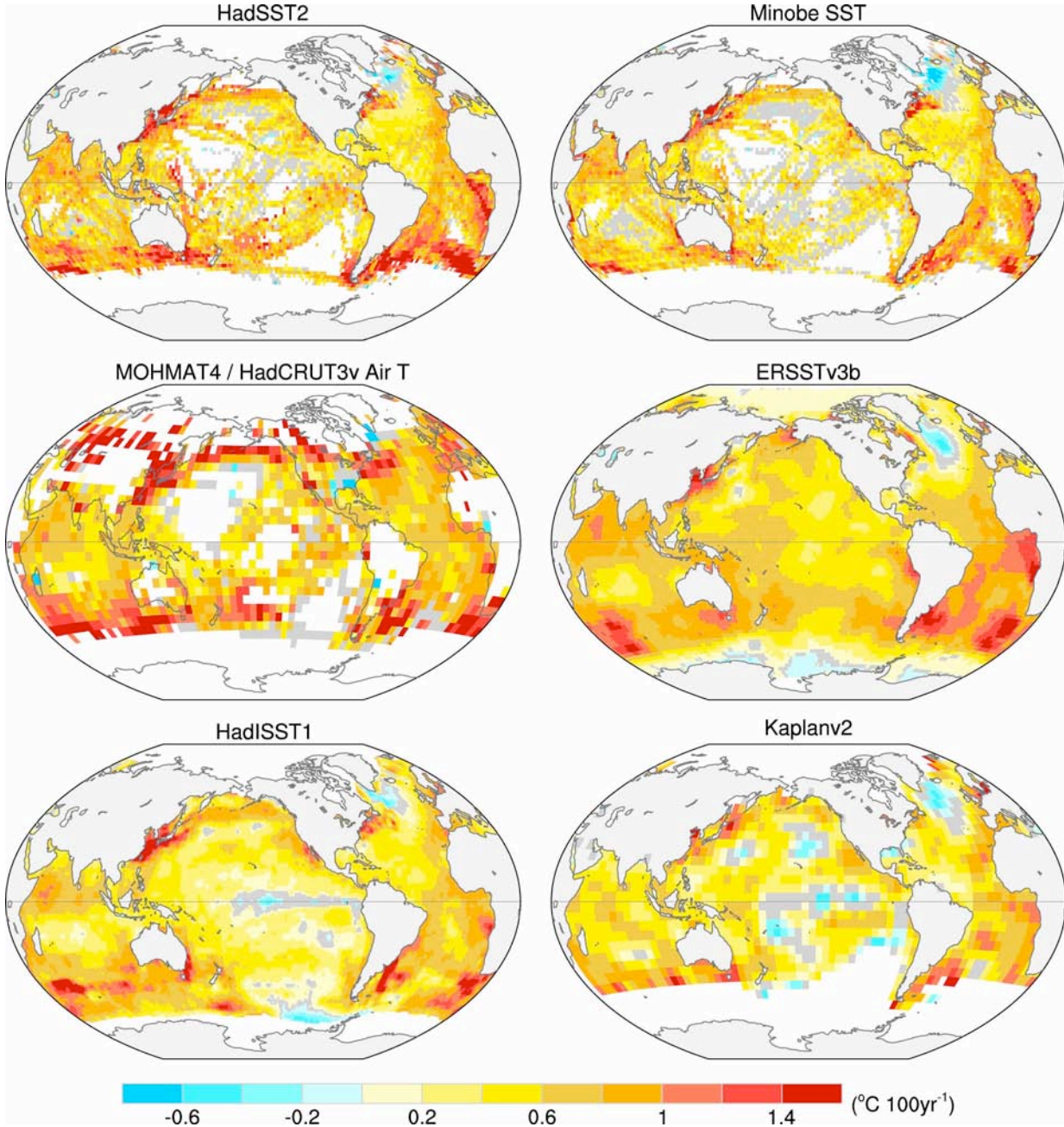


Figure 11. Observed twentieth century SST trends ($^{\circ}\text{C}$ per century) computed from monthly anomalies since 1900 using various SST datasets. White grid boxes denote insufficient data, and gray boxes indicate trends that are not statistically significant at the 95% confidence level (from Deser et al., 2010).

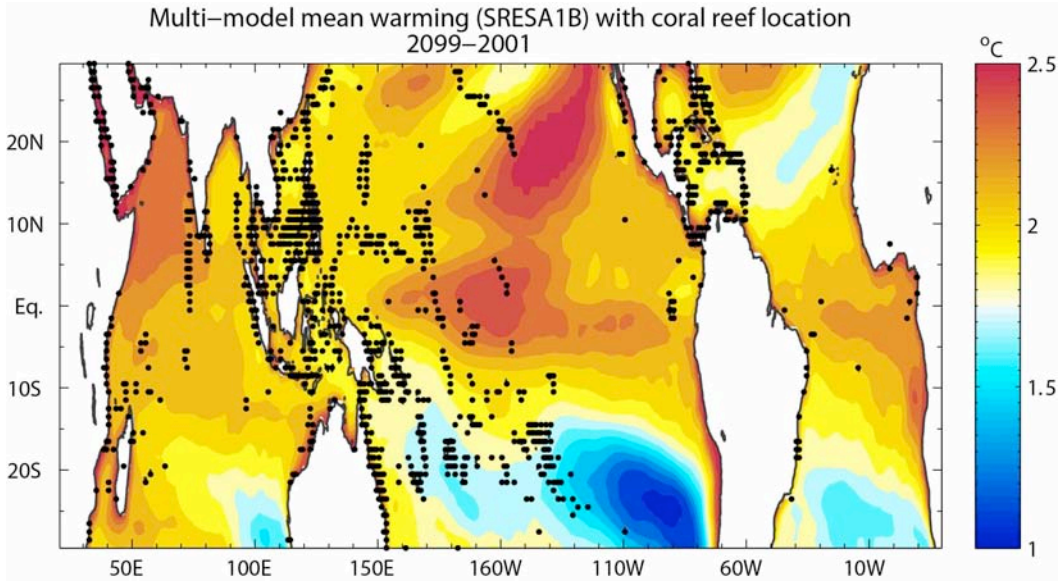


Figure 12. SST change over the twenty-first Century, averaged over 22 climate models for a mid-range emissions scenario (SRES A1B). Reef locations are indicated by black circles (data from www.reefbase.org) (from Clement et al., 2010).

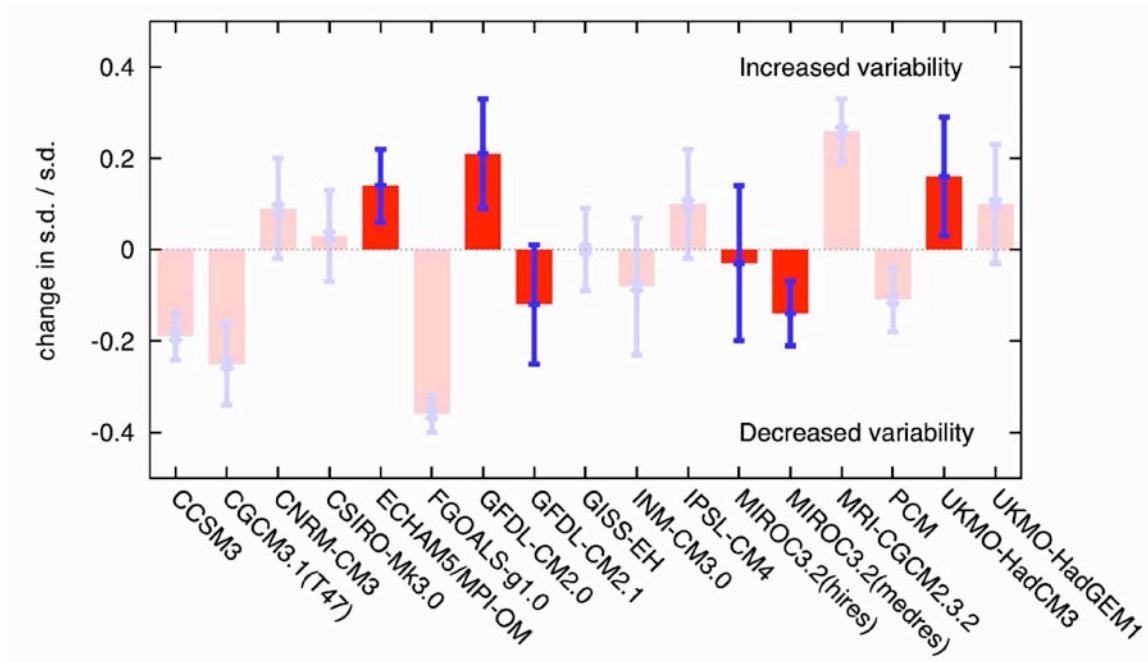


Figure 13. Projected changes in the amplitude of ENSO variability, as a response to global warming, from the CMIP3 models. The measure is derived from the interannual standard deviation (s.d.) of a mean sea-level-pressure index, which is related to the strength of the Southern Oscillation variations. Positive changes indicate a strengthening of ENSO, and negative changes indicate a weakening. Statistical significance is assessed by the size of the blue bars, and the bars indicated in bold color are from those CMIP3 CGCMs that are judged to have the best simulation of present-day ENSO characteristics and feedbacks (from Collins et al., 2010).